Spatio-Temporal Changes of Snow Cover and Its Relationship With Meteorological Factors on the Qinghai-Tibet Plateau, China

Haoyu Jin
Sun Yat-Sen University
xiaohong chen (eescxh@mail.sysu.edu.cn)
Center for Water Reources & Environment, Sun Yat-sen Univeristy

Research Article

Keywords: snow melt day, snow cover ratio, glacier, climate change, Tibetan Plateau

Posted Date: April 27th, 2021

DOI: https://doi.org/10.21203/rs.3.rs-453378/v1

Spatio-temporal changes of snow cover and its relationship with meteorological factors on the Qinghai-Tibet Plateau, China

Haoyu Jin[1, 2, 3] · Xiaohong Chen[1, 2, 3, *]

[1] Center for Water Resources and Environment, Sun Yat-sen University, Guangzhou 510275, China

[2] Guangdong Engineering Technology Research Center of Water Security Regulation and Control for Southern China, Sun Yat-sen University, Guangzhou 510275, China

[3] Key Laboratory of Water Cycle and Water Security in Southern China of Guangdong High Education Institute, Sun Yat-sen University, Guangzhou 510275, China

[*] Corresponding author. E-mail address: eescxh@mail.sysu.edu.cn (X. Chen).

Received date; accepted date

Abstract

The Qinghai-Tibet Plateau (TP) is one of the most sensitive areas to climate change, and its ecological environment changes directly or indirectly reflect the global climate change trend. The snow cover ratio (SCR) is an important indicator reflecting the climate and environmental changes of the TP. The daily remote sensing data of snow cover on the TP from 2003 to 2014 were used to study the spatio-temporal distribution of snow cover on the TP. The results have shown that the average snowmelt day on the TP starts on the 103rd day and ends on the 223rd day of a year, and the snowmelt duration has a downward trend. Snow is mainly distributed in the Nyainqentanglha Mountains, Karakoram Mountains and Himalayas. The SCR in summer has a downward trend, while in autumn has a rising trend. This shows that the difference in SCR during the year has enlarged, increasing the risk of snowmelt floods. The SCR is highly correlated with temperature, but weakly correlated with precipitation. Using the long-term remote sensing data of snow cover, the distribution of glacier coverage on the TP can be extracted, in which glaciers on the TP account for about 1%. This research provides an important reference for in-depth understanding of the snow cover changes on the TP and their impact on the environment.

Keywords snow melt day · snow cover ratio · glacier · climate change · Tibetan Plateau

1 Introduction

Snow is an important component of the cryosphere(Gao et al., 2021; Shijin et al., 2019; Wang et al., 2019). Its high reflectivity, low thermal conductivity and snowmelt effect have a significant impact on atmospheric circulation, land surface hydrological processes and regional water balance(Liu et al., 2021; Teng et al., 2021; Wen et al., 2019; J. Zhang et al., 2021). In climate change research, snow cover is a key climate variable, and its seasonal variation is the most significant factor leading to changes in surface albedo, which in turn causes the balance of earth and gas energy and regional

level thermal differences(Cha et al., 2014; Yi et al., 2021; Yu et al., 2018; H. Zhang et al., 2021; W. Zhang et al., 2021). It has an important impact on local and even global climate change, and at the same time is very sensitive to climate change(Achugbu et al., 2021; Jia et al., 2021; Poudyal et al., 2021). In the global water cycle, the accumulation and melting of snow plays a role in the redistribution of water during the year, and is the most important freshwater resource in spring in arid and semi-arid regions(Fan et al., 2015; Saarnio et al., 2018; Wu et al., 2018; Zhu et al., 2021). 10% of the global land surface is covered by permanent glaciers and snow, 34% of the area has seasonal snow, and the average snow coverage in the northern hemisphere is about 0.07% to 4.00%(Ahluwalia et al., 2021; Sobota et al., 2020; Thind et al., 2021). In the past 30 years, the area of snow in cold regions has been decreasing(Konya et al., 2020). The snow and ice surface of Antarctica continues to shrink, the snow cover of the Antarctic continental coastal zone shows a fluctuating decrease, and the snow coverage of the Arctic also shrinks continuously(Jabbar et al., 2020; Niu et al., 2020; Sood et al., 2020). The accelerated melting of glaciers has brought huge challenges to the global climate and environment, and has become a hot spot in climate change research in recent years(Chen et al., 2019; Pu et al., 2020; Thapa et al., 2020).

Due to geological processes, the TP has formed a huge uplift(Sun et al., 2019). Even in the middle and low dimensions, the TP presents a cold climate due to its high altitude(Zhou et al., 2018). The TP is a sensitive area to climate change. Snow is the most active natural factor on the underlying surface of the TP, and it is the link between the plateau environment and climate(Jiang et al., 2020; Li et al., 2021). It has an important impact on regional climate change and the evolution of ecological environment by changing the surface radiation and atmospheric heat circulation(B. Zhang et al., 2020). At the same time, there are abundant water resources in glaciers and snow, which are an important water supply for rivers and affect the regional surface water cycle, water resources distribution, and local production and life(Zhu et al., 2012). At present, research on snow cover mainly focuses on the temporal and spatial changes of snow cover, changes in snow cover trends, snow depth and snow line, snow albedo and snow melting mechanism(Dong et al., 2020; Farrington and Tsering, 2019; Yang et al., 2020; Zhao et al., 2018).

The data for studying snow cover is mainly ground station observation data and satellite remote sensing data. Because of its wide coverage, strong consistency and high spatial resolution, remote sensing data has become the mainstream data for studying snow cover(Tong et al., 2020). The ground station data is usually used as verification data to analyze the quality of remote sensing data products(Hall et al., 2021). Satellite remote sensing monitoring of snow can be divided into two types: microwave remote sensing and visible light remote sensing(X. Zhang et al., 2020). The former mainly uses the penetration ability of microwave signals to ground objects to monitor the depth and density of snow, while the latter mainly uses the optical characteristics of snow in visible light and near infrared light to monitor the snow cover area and its spatial changes(Tong et al., 2020). The most widely used snow cover datasets are Suomi National Polar-orbiting Partnership (NPP) snow cover suite, Moderate-Resolution Imaging Spectroradiometer (MODIS) snow cover products, and

European Space Agency (ESA) Global Snow Monitoring for Climate Research (GlobSnow) and so on(Steele et al., 2017; Tang et al., 2020; Zhang et al., 2019).

In this study the long time series data of snow cover area on TP (2003-2014) dataset was used to analyze the annual snow cover change, monthly snow cover change, seasonal snow cover change, and correlation of snow cover with meteorological factors. Furthermore, snow cover data was used to analyze the start time and end time of snowmelt and extract glacier-covered areas.

2 Study area

The TP is called the third pole of the earth due to its cold natural environment. Because it is the birthplace of many major rivers in Asia, such as the Yangtze River, Yellow River, Yarlung Zangbo River, Lancang River, etc., it is also called the Asian Water Tower. The geographical location of the TP is between 26°00′10″N-39°04′25″N, 73°03′37″E-104°07′59″E, with an area of 2.62 million km^2. The TP is surrounded by high mountains, with plateaus, basins and deep-cut canyons in the middle (Fig. 1). It extends from the Karakoram Mountains in the west, the Himalayas in the southwest to the Hengduan Mountains in the southeast, and reaches the northern edge of the Qilian Mountains, Altun Mountains and Kunlun Mountains in the north. The terrain is steep, changeable and complex, with an average elevation of about 4378 m a.s.l.(Gao et al., 2021).

The regional climate types of the TP are complex and diverse(J. Zhang et al., 2021). The climate zones are mainly plateau temperate zone, plateau sub-frigid zone and plateau frigid zone. Vegetation types change significantly with elevation and climatic zones, and there are significant horizontal and vertical zoning characteristics in spatial distribution, mainly including alpine shrubs, alpine grasslands and meadows. The TP has long and cold winters, short warm summers, and large temperature difference between day and night. The annual average temperature decreases from 20°C in the southeast to below -6°C in the northwest. As the warm and humid air currents in the southern ocean are blocked by multiple high mountains, the annual precipitation also decreases from 2000 mm to less than 50 mm. The precipitation is most concentrated in May to September and its spatial distribution is extremely uneven. The snowfall starts in September, and the obvious snow cover period is from September to April of the following year. The TP is also facing environmental problems such as glacier melting, land desertification, and soil erosion. It is an area highly sensitive to global climate change.

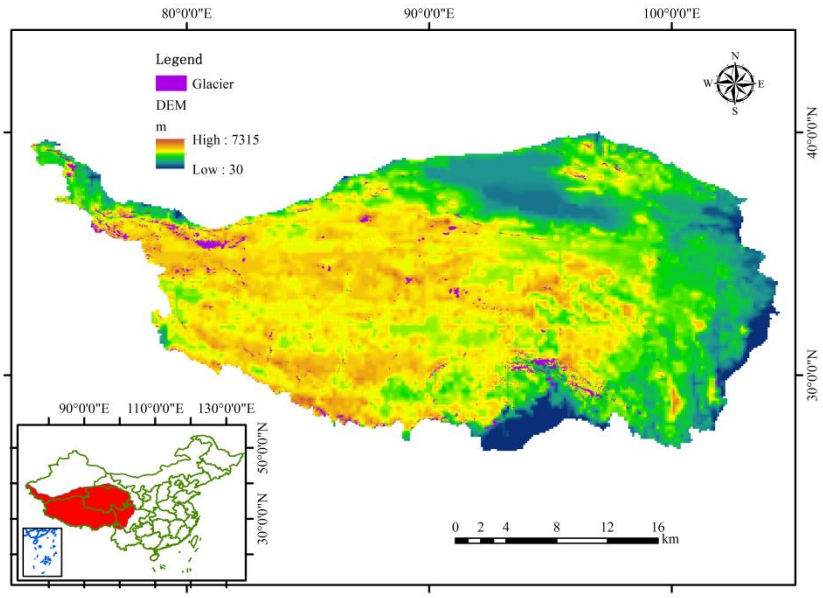

Fig. 1 Location of study area and distribution of glaciers

3 Materials and methodology

3.1 Datasets

We used the Long time series data of snow cover area on Qinghai-Tibet Plateau (2003-2014) dataset, which was downloaded from the National Tibetan Plateau Data Center (NTPDC) (http://data.tpdc.ac.cn)(Xiaohua, 2019). The dataset is a combination of MODIS (version 005) and Ice Mapping System (IMS) datasets, and the interpolated cloud removal algorithm is used for cloud removal processing to obtain a daily snow-covered area cloudless product. The spatial resolution is 0.005 degrees and the temporal resolution is daily. The glacier catalog data of the Qinghai-Tibet Plateau is extracted from the complete catalog dataset of global glacier contours released by Global Land Ice Measurements from Space (GLIMS) (http://www.glims.org/RGI/).

3.2 Snow cover days

Snow cover days (SCD) describes the number of times each pixel is covered by snow in a certain period of time. The larger the number of snow cover days, the longer the snow cover in the area and the more abundant the snow storage.

$$SCD = \sum_{i=1}^{N} S_i \quad (1)$$

Where *SCD* is the snow cover days, *N* is the total duration time, S_i is the judgment value of daily snow cover for a certain pixel, 1 for snow cover and 0 for no snow cover.

3.3 Snow cover ratio

The snow cover ratio (SCR) indicates the ratio of the snow cover time of a certain pixel to the total time. The formula is calculated as follows:

$$SCR = \frac{S_{time}}{T_{total}}$$

Where S_{time} is the duration time of snow cover, T_{total} is the total duration time.

4 Results

4.1 Snowmelt duration time

Snow melting time is an important indicator to measure the change state of snow cover. The moving average (MA) algorithm was used to eliminate the abrupt changes in the original snow cover sequence. Combining the image and the actual situation, the time points when the snow cover starts/stops to melt are extracted from the moving average curve. Fig. 2 illustrates the changes in the daily snow cover area of the TP from 2003 to 2014. It can be seen from the figure that the snow cover area of the TP has a change process from high to low and then increases. Generally, the snow cover area is at a high level from September to March of the following year. Snow melting starts around April and continues until around August. The snow cover area changes in a zigzag pattern, and each snowfall causes the snow cover area to increase suddenly. The vertical lines indicate the starting point and ending point of continuous ablation of the snow cover, which is extracted by the changing points of the MA curve.

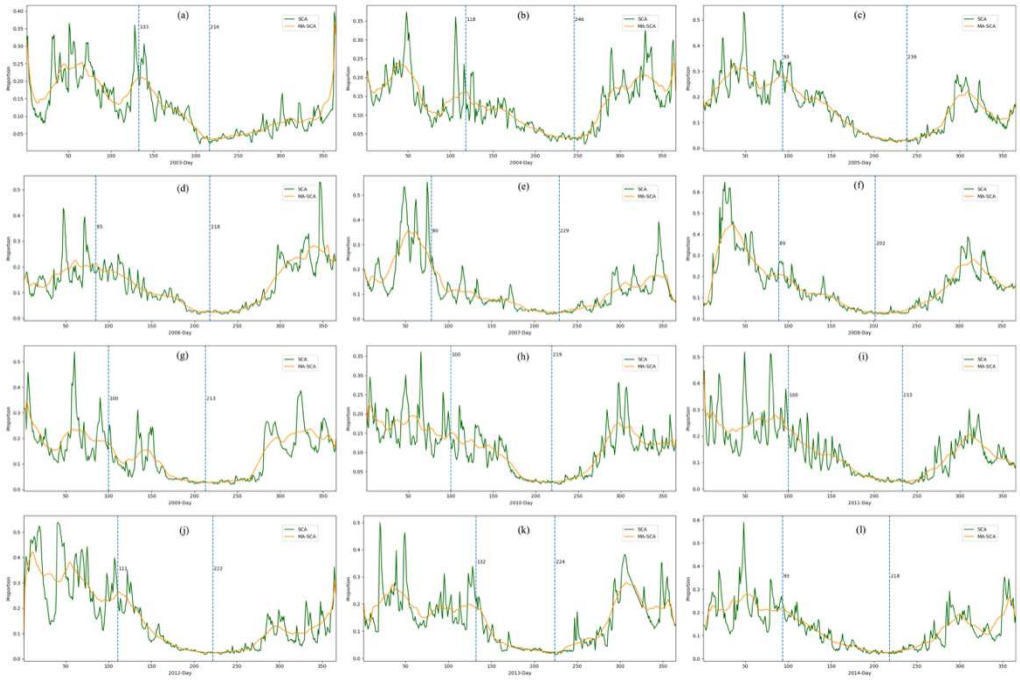

Fig. 2 Changes in daily snow cover area of the TP from 2003 to 2014 (a-l: 2003-2014)

Fig. 3 a illustrates the change of snow melting period from 2003 to 2014. In summary, the start time of snow ablation has a trend from being late to early and then later, and the end time of snow ablation has a trend from being late to early and then later. The average snowmelt time starts on the 103rd day of each year, which is around early April. The average snowmelt time ends on the 223rd day of each year, which is around early August. Fig. 3 b illustrates the number of days in the snow melting period and its changing trend from 2003 to 2014. It can be seen from the figure that the snow melting period was the shortest in 2003, which was 84 days. In 2007, the snow melting period was the longest, reaching 150 days. The average number of snow melting days is 121, and the snow melting days have a slight tendency to shorten.

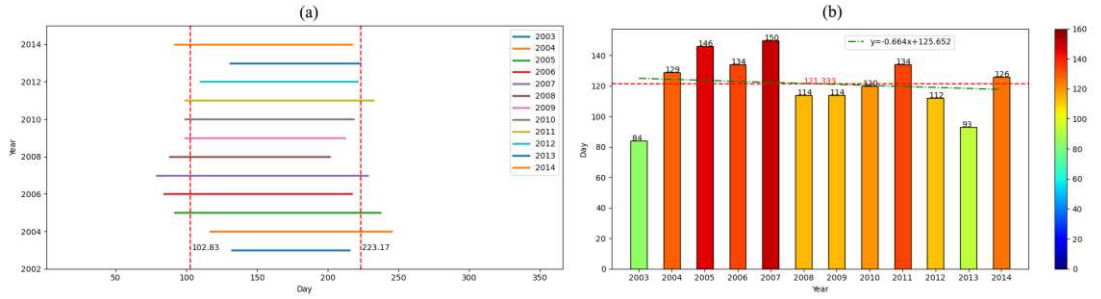

Fig. 3 Snowmelt duration time (a) and change trend (b) from 2003 to 2014

4.2 Annual SCR change

Fig. 4 illustrates the change of SCR from 2003 to 2014. From the figure, it can be seen that the annual SCR fluctuates and the cycle is about 4 years. The SCR was the highest in 2008, reaching 0.164. In the same year, southern China suffered a snow disaster, which shows that the snowfall on the TP is consistent with the snowfall in southern China. In 2010, the SCR was the lowest, only 0.114. The multi-year average SCR is 0.141, and the SCR shows a slight upward trend.

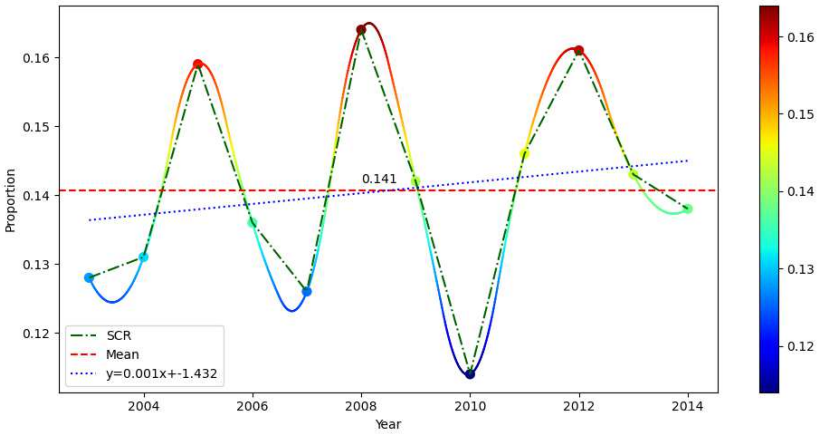

Fig. 4 Changes in the average annual SCR from 2003 to 2014

5 illustrates the change in the distribution of the average annual SCR on the TP from 2003 to 2014. It can be seen from the that most areas have SCR less than 0.2. The main areas of high SCR are Nyainqentanglha Mountain, Karakoram Mountain, and the northern foot of the Himalayas. There were many areas with high snow coverage in 2008, while the least in 2010. Areas with extremely high SCR are generally permanent glaciers. The Karakoram Mountains, for example, have widespread glaciers. The reason for the high SCR in the southwestern TP is that there is plenty of water vapor and the temperature on the high mountains is low enough to produce snow easily. Although the temperature in the northwest TP is low, the water vapor is low, thus resulting in less snow.

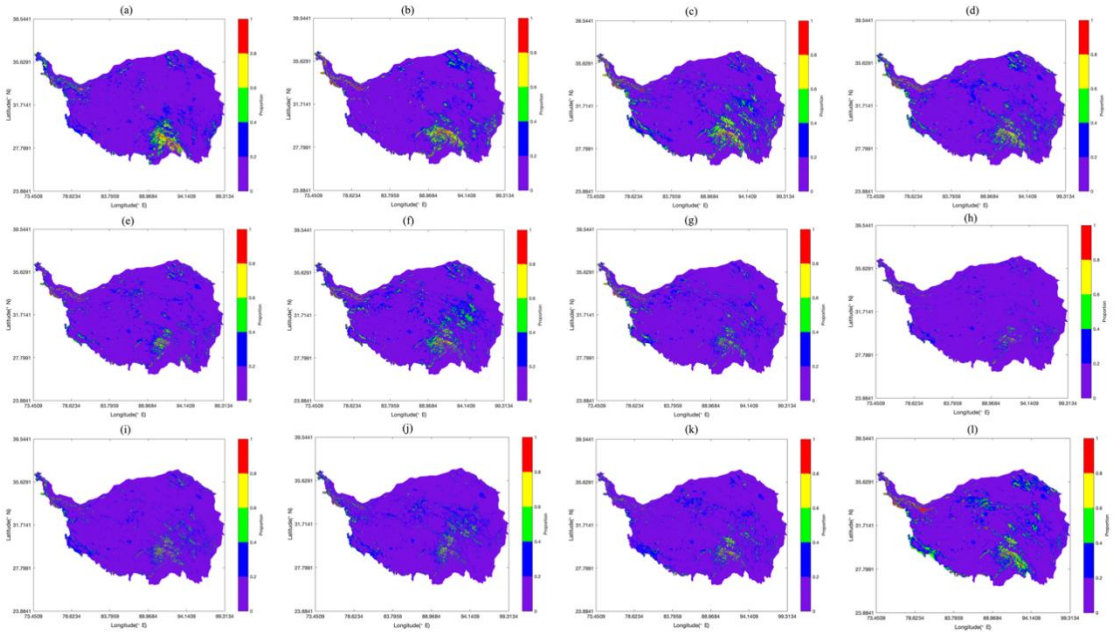

Fig. 5 Distribution of average annual SCR from 2003 to 2014 in the TP (a-l: 2003-2004)

The number of SCD is similar to the spatial distribution of SCR. Generally, areas with high SCR have more SCD. Fig. 6 illustrates the spatial distribution of the number of SCD on the TP from 2003 to 2014. It can be seen from the figure that in the Nyainqentanglha Mountains, the Karakoram Mountains and the Himalayas, the annual SCD are more than 140 days, and some areas are covered with snow throughout the year. The SCD in most areas are less than 70 days, mainly in the Qiangtang Plateau in the northwest of the Qinghai-Tibet Plateau. The changes in high and low snow cover areas are relatively stable. Generally, in years with a high number of snow cover days, snow cover mainly increases in the northeastern TP.

Fig. 7 illustrates the spatial distribution of the multi-year average SCR and SCD of the TP. From Fig. 7 a, it can be seen that the SCR of 85% of the TP is less than 0.18. The main areas with high SCR are concentrated in the southeast mountainous areas, such as the Nyainqentanglha Mountain, Hengduan Mountain and Bayan Har Mountain. As for the Karakoram Mountains in the west, the northern foothills of the Himalayas in the southwest, and the southern foothills of the Qilian Mountains in the northwest, these areas are mainly distributed with glaciers. From Fig. 7 b, it can be

seen that areas with high SCR generally have more SCD. The days of high SCD are mainly concentrated in the Nyainqentanglha Mountains, Karakoram Mountains and Himalayas.

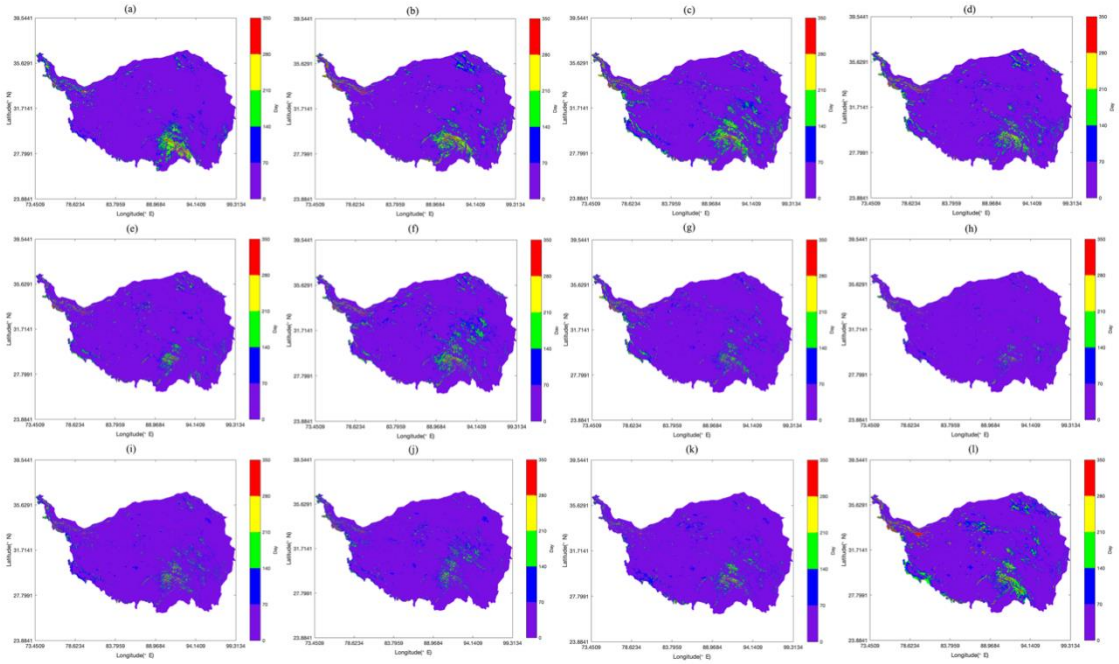

Fig. 6 Spatial distribution of annual SCD on the TP from 2003 to 2014 (a-l: 2003-2014)

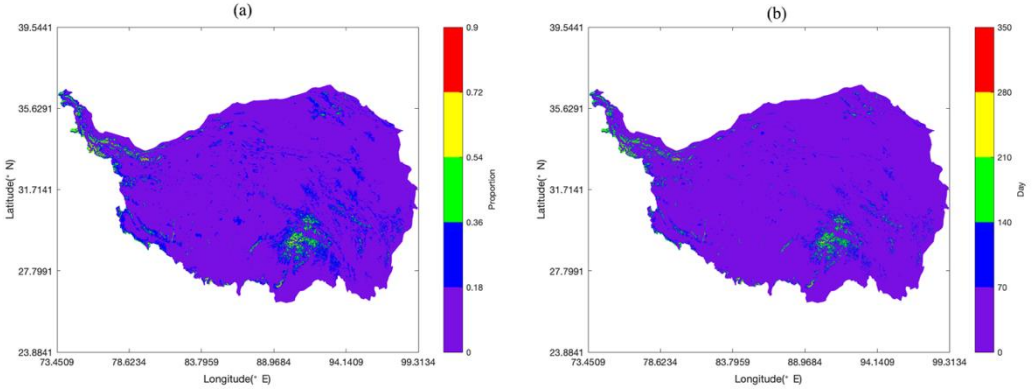

Fig. 7 Spatial distribution of the multi-year average SCR (a) and SCD (b) on the TP

4.3 Monthly SCR change

Fig. 8 illustrates the monthly SCR changes from 2003 to 2014. It can be seen from the figure that the monthly SCR of the TP is U-shaped. The months with high SCR are January, February, March, April, November, and December. Meanwhile the SCR is low in July, August and September. May and June are periods of rapid snow melting, and October is a period of rapid accumulation of snow. In general, February has the highest SCR, and August has the lowest SCR. These are also the two months with the lowest and highest average temperature on the TP, indicating a strong correlation between SCR and temperature.

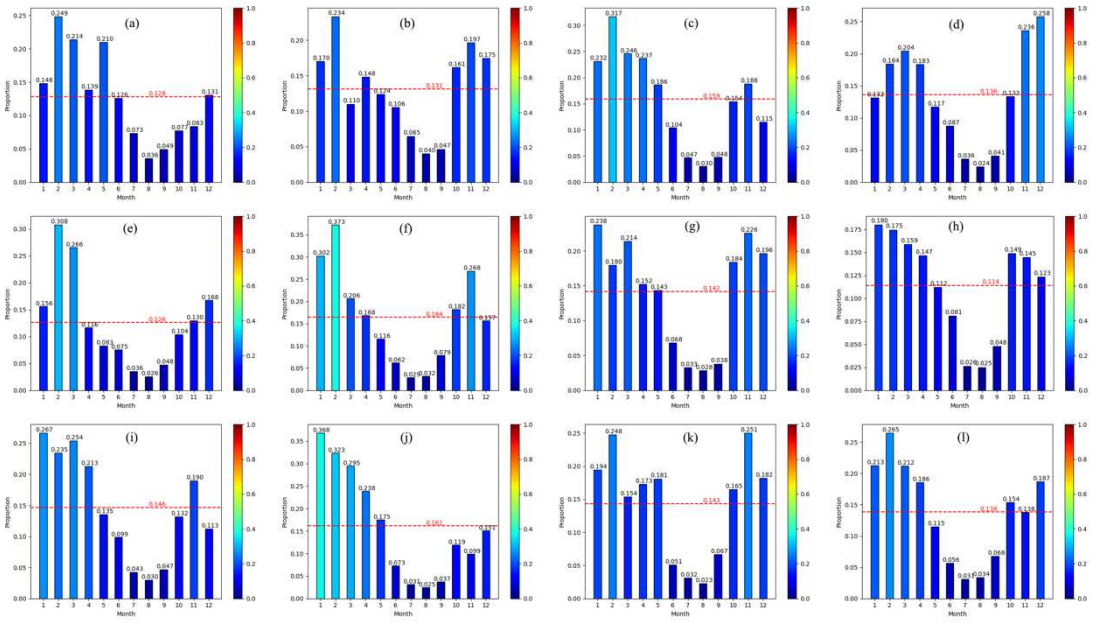

Fig. 8 Monthly SCR change from 2003 to 2014 (a-l, 2003-2014)

Fig. 9 illustrates the monthly SCR changes from 2003 to 2014. It can be seen from the figure that the SCR changes steadily in February, November and December, with no obvious trend of change. In January, March, April, September and October, the SCR has an upward trend. In May, June, July and August, the SCR has a decreasing trend, especially in June, where the decreasing trend is the fastest. This shows that the snow cover rate of the TP is more differentiated during the year, and the SCR is developing in a trend of steep rise and fall. The climatic environment has become more differentiated.

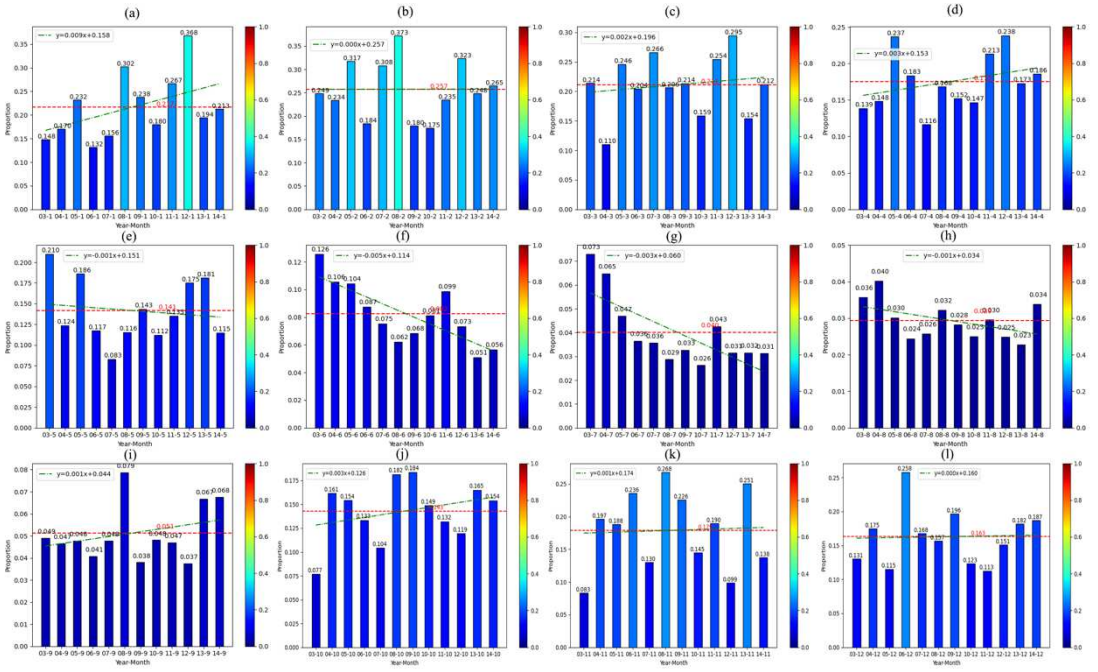

Fig. 9 Changes in SCR of TP from January to December (a-l: Jan-Dec)

Judging from the changes of monthly average SCR (Fig. 10), February has the highest SCR and August has the lowest SCR. The monthly average SCR is 0.141. The SCR in January, February, March, November and December is higher than the average level. The SCR in May and October is close to the average level, while in June, July, and August , September it is below average. Snow melts mainly in May and June, and accumulates in September and October.

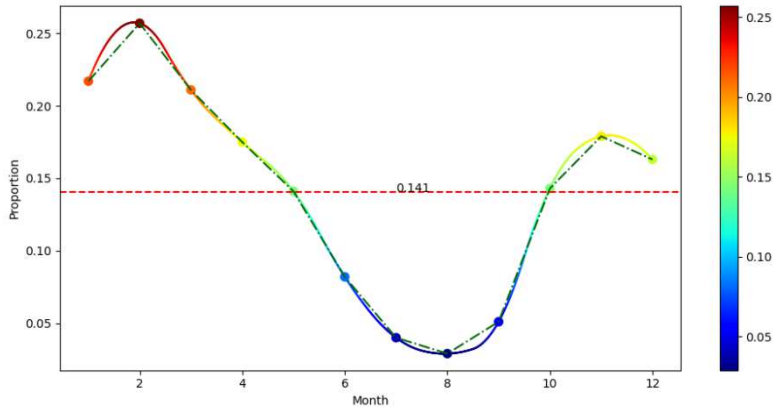

Fig. 10 Changes in monthly average SCR on the TP

Fig. 11 illustrates the spatial distribution characteristics of the monthly average SCR. It can be seen from the figure that the TP is in a period of high SCR in January, February, March, November and December. The snow is mainly concentrated in the Nyainqentanglha Mountains, Karakoram Mountains, Himalayas, Bayan Har Mountains, Qilian Mountains and other high mountains. Among them, Nyainqentanglha Mountain is the most concentrated area of snow. In June, July, August, and September, the snow melts in most areas, and the areas with snow cover are mainly permanent glaciers. The SCR decreases in the fastest speed in April and May, which is the main snowmelt period. The SCR increases in the fastest speed in October, which is the main snow cover period.

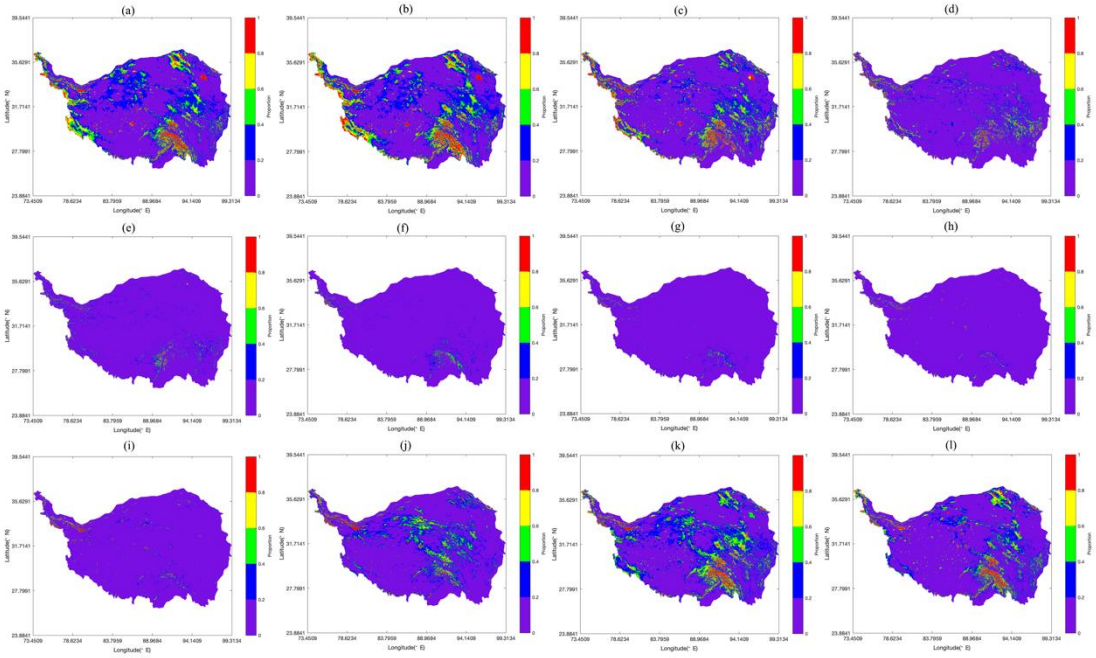

Fig. 11 Spatial distribution of monthly average SCR on TP from January to December (a-l: Jan-Dec)

4.4 Seasonal SCR change

Fig. 12 illustrates the changes of SCR in four seasons from 2003 to 2014. It can be seen from the figure that the SCR is generally highest in winter and spring, followed by autumn, and the lowest in summer. Snow melts from spring to summer, and accumulates from autumn to winter. Although the average SCR was the highest in 2008, 2012 was the highest in spring, 2007 was the highest in winter, and 2003 was the highest in summer. This shows that even in years with relatively normal annual SCR, the seasonal SCR may be abnormal.

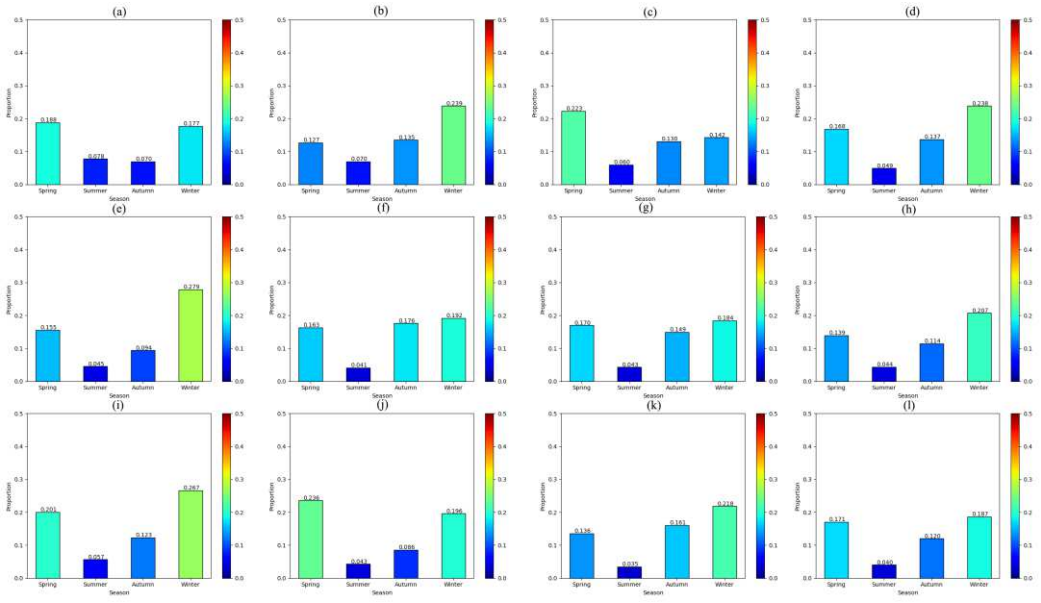

Fig. 12 Seasonal change of SCR on TP from 2003 to 2014 (a-l: 2003-2014)

Fig. 13 illustrates the change of SCR in the four seasons of spring, summer, autumn and winter from 2003 to 2014. It can be seen from the figure that the SCR of the TP is high in winter and spring, when the trends of SCR are not obvious and the state is relatively stable. On the TP, the SCR is decreasing in summer, while increasing in autumn. This shows that the seasonal SCR of the TP has become more differentiated, with accelerated melting of snow from spring to summer, and a rapid increase in snow from autumn to winter. This also indirectly indicates that the seasonal climate of the TP is changing.

The spatial distribution of the average spring, summer, autumn and winter SCR over the years is shown in Fig. 14. It can be seen from the figure that the TP has the highest SCR in winter and the lowest in summer. The main areas covered by snow in winter are the Nyainqentanglha Mountains, Karakoram Mountains, Himalayas, Bayan Har Mountains, Qilian Mountains and other high mountains. In summer snow mainly covers the Nyainqentanglha Mountains, the Karakoram Mountains, and the Himalayas, mainly because there are glaciers in these areas. The SCR in spring is

wide, but it is scattered, and the SCR in autumn is significantly larger than that in summer.

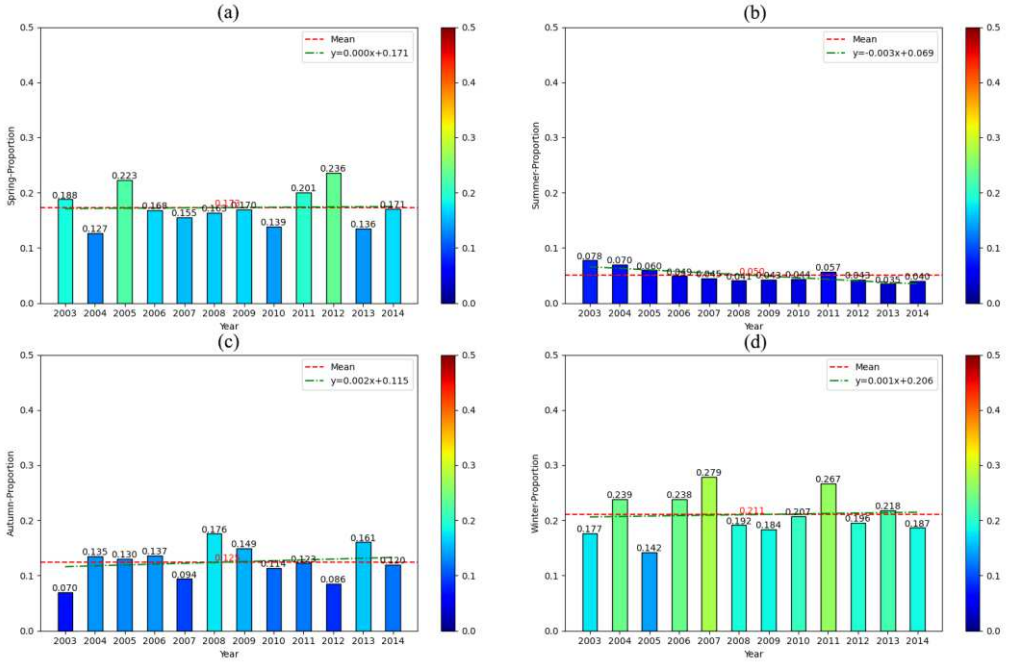

Fig. 13 Changes in SCR of the TP from 2003 to 2014 in spring (a), summer (b), autumn (c) and winter (d)

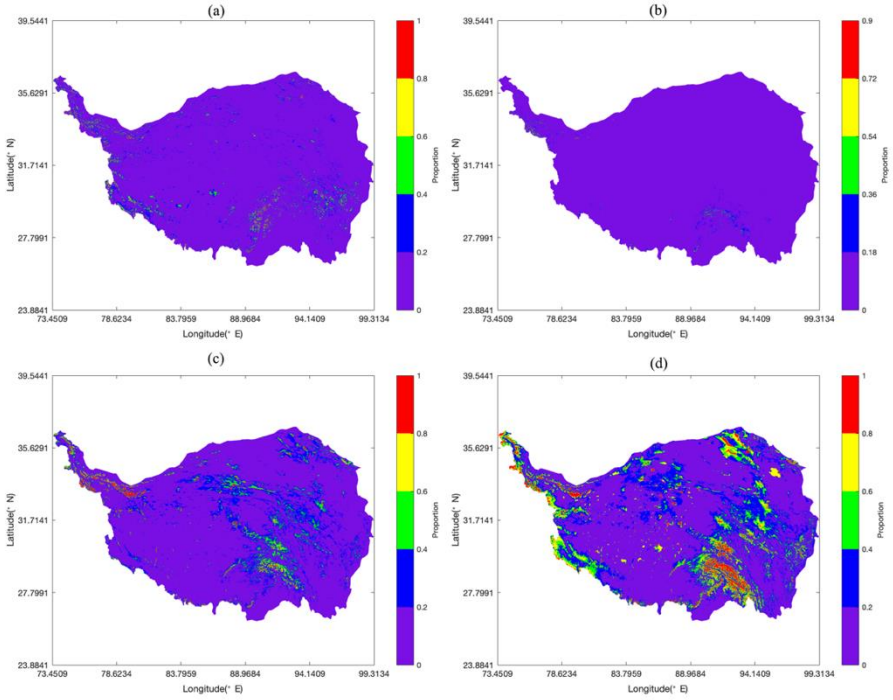

Fig. 14 Spatial distribution of average SCR in spring (a), summer (b), autumn (c) and winter (d) on the TP

4.5 Relationship of SCR with precipitation and temperature

The annual precipitation distribution on the TP presents an obvious cascade distribution, decreasing from southeast to northwest. Southern Tibet, the lower reaches of the Yarlung Zangbo River, and the Hengduan Mountains have a lot of precipitation, while the Qiangtang Plateau has sparse precipitation, with annual precipitation less than 300 mm. Among them, 2008 has witnessed a wide area of large precipitation, which is also the year with high SCR, while 2010 is a year with large precipitation distributed in a small area, which is the year with low SCR. This indicates that if there is more precipitation in a year, there will be more snow. In addition, there is an increasing trend in areas with heavy rainfall in the southeast of the TP. It is worth noting that in the Karakoram Mountains, although there is not much precipitation, there is a large amount of snow cover, which is mainly due to the widespread distribution of permanent glaciers in this area.

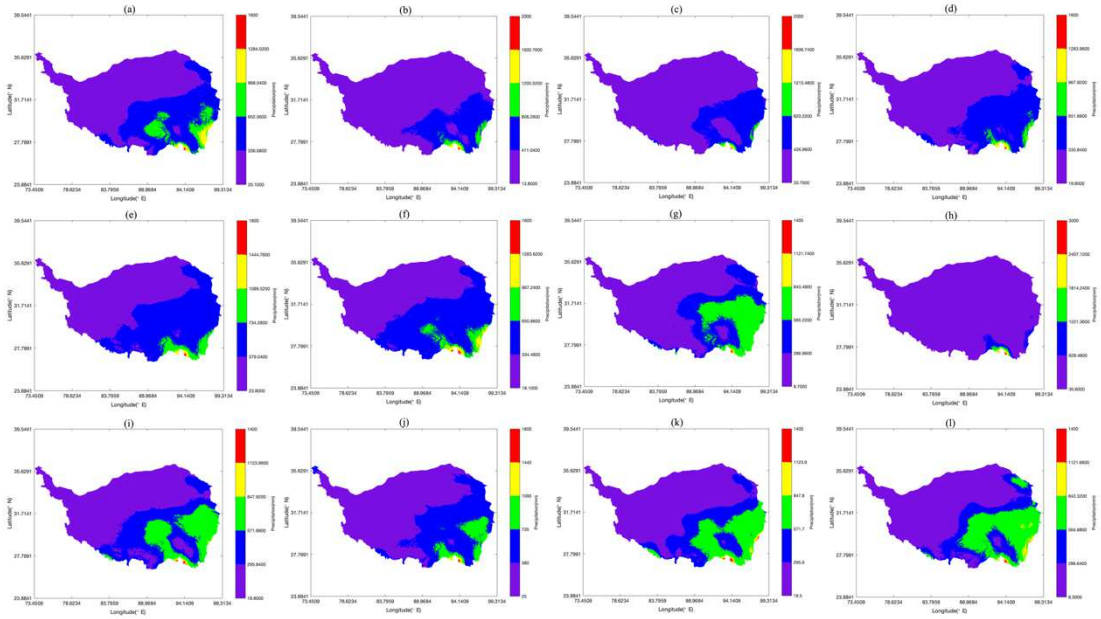

Fig. 15 Spatial distribution of annual precipitation on the TP from 2003 to 2014 (a-l: 2003-2014)

The average annual temperature distribution on the TP is roughly in three levels (Fig. 16). The area with the highest temperature is southern Tibet, the area with the lowest temperature is the Qiangtang Plateau, and the temperature in other areas is somewhere in between. Although the precipitation in southern Tibet is heavy, the temperature is high, making the precipitation mostly in the form of rainfall. Therefore there is little snow in this area. Although the temperature in the Qiangtang area is low, the precipitation is scarce. Thus the snow cannot accumulate. Even if there is snow, it will quickly evaporate. The Nyainqentanglha Mountain and the Hengduan Mountains have low temperature and relatively high precipitation. The main form of precipitation is snowfall, making these areas the most snow-covered areas.

Fig. 17 a illustrates the changes in SCR and annual precipitation from 2003 to 2014. It can be seen from the figure that the annual precipitation trend is not obvious, while the SCR fluctuates. From the analysis results of the correlation between precipitation

and SCR (Fig. 17 c), the correlation between precipitation and SCR is 0. Fig. 17 b illustrates the change in SCR and annual average temperature from 2003 to 2014. It can be seen from the figure that the SCR is low in the year with high temperature, and is high in the year with low temperature. The SCR is negatively correlated with temperature (Fig. 17 d), and the correlation is obvious, with a correlation coefficient of 0.269.

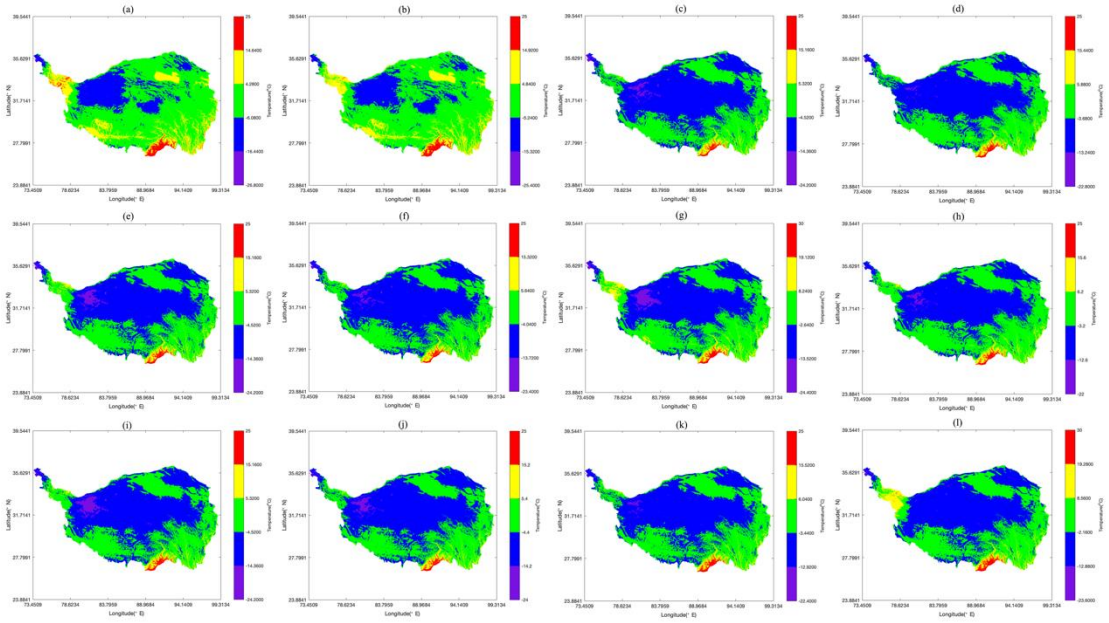

Fig. 16 Spatial distribution of annual average temperature on the TP from 2003 to 2014 (a-l: 2003-2014)

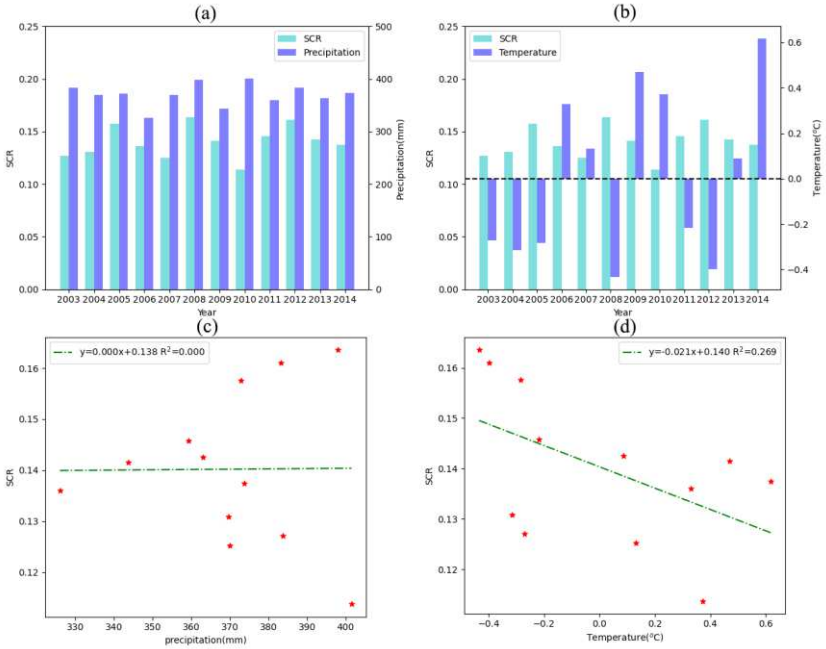

Fig. 17 Changes of SCR with precipitation (a) and temperature (b) from 2003 to 2014, and correlations of SCR with precipitation (c) and temperature (d)

4.6 Distribution of glaciers on the TP

The Qinghai-Tibet Plateau and the marginal mountains are the most concentrated areas of glaciers. Using Randolph Glacier Inventory (RGI) released by GLIMS, the distribution of glacier cover on the Qinghai-Tibet Plateau is shown in Fig. 18 a. It can be seen from the figure that glaciers are mainly distributed in the Nyainqentanglha Mountains, Karakoram Mountains, Himalayas, Qilian Mountains and other regions. The glacier coverage in the Karakoram area reaches 23.42%. Fig. 18 b is the glacier-covered area obtained by statistics of snow cover. The area with a snow cover rate greater than 0.9 is regarded as a glacier. Compared with Fig. 18 b, the glacier data obtained through the snow cover data is more accurate, and the main glacier-covered areas can be extracted. Glacier coverage on the Qinghai-Tibet Plateau is about 1.08%. It provides a reference for the extraction of glacier cover.

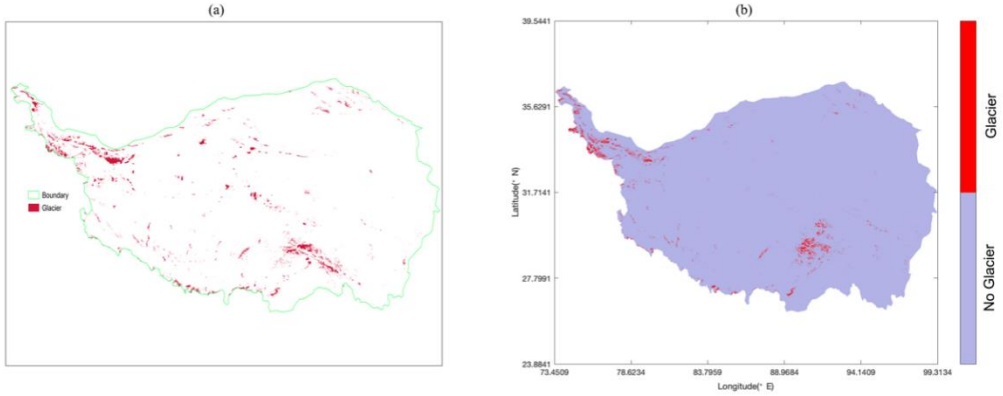

Fig. 18 Glacier cover on the TP based on RGI (a) and SCR (b)

5 Discussion

Snow and glaciers are an important part of the hydrological cycle of the TP(Sun et al., 2019; Thind et al., 2021; Zhou et al., 2018). Changes in snow cover not only affect the natural environment of the TP, but also have an important impact on regional water resources(Konya et al., 2020; Sood et al., 2020). The typical snow melting process includes accumulation, early snow melting and snow melting period(Thapa et al., 2020). A sudden large-scale snowmelt process will trigger snowmelt floods(Chen et al., 2019). Studies have found that the snowmelt period of the TP is shortening, which will increase the probability of snowmelt floods and thus is worthy of vigilance(Li et al., 2021; Sun et al., 2019). Runoff simulation in plateau mountainous areas needs to be combined with models that consider snowmelt runoff(Yang et al., 2020). Previous studies have found that the Yarlung Zangbo River snow melt water accounts for 9.7% of the total runoff, the source area of the Yangtze River accounts for 13.6%, and the upper reaches of the Heihe River accounts for 16.1%(Sobota et al., 2020). This shows that the snowmelt runoff mechanism in the TP is obvious, and the impact of snow and glaciers on the hydrological cycle needs to be considered.

Although the correlation between precipitation and SCR is 0 throughout the TP, it cannot be denied that the correlation between precipitation and SCR is very high in some areas. For example, the Nyainqentanglha Mountain area has a lot of precipitation, which makes the SCR high, and the Qiangtang Plateau has less precipitation, which makes the SCR low. In this study, the TP was taken as a whole to analyze the relationship between precipitation and SCR, which will obscure some local information. In future research, the TP can be divide into different regions for study.

6 Conclusions

Glaciers and snow are the most common natural landscapes on the TP, and they are also important indicators of climate and environmental changes. Based on remote sensing data of snow cover on the TP, this study analyzed the snow-melting period, yearly, monthly, and seasonal changes of SCR and the distribution of glaciers on the TP. It provides an important reference for the comprehensive understanding of the snow cover change law of the TP . Main conclusions drawn from this study are as follows:

(1) The average snowmelt on the TP begins on the 103rd day of the year, which is early April, and the snowmelt ends on the 223rd day, which is early August. The average snowmelt duration is 121 days, and the snowmelt time has a tendency to shorten.

(2) The annual SCR fluctuates, and the main snow cover areas are the Nyainqentanglha Mountains, Karakoram Mountains, and Himalayas. The SCR decreases in May, June, July, and August, while it increases in April, indicating that snow melting on the TP is accelerating. This is also reflected in the decrease in SCR in summer and the increase in SCR in autumn, indicating that the difference in SCR on the TP has enlarged during the year.

(3) The SCR of the TP is negatively correlated with temperature, but weakly correlated with precipitation. However, there are differences in the correlation between precipitation and SCR in different partial areas. Using remote sensing data of long-term snow cover, the distribution of glacier cover on the TP can be extracted, which is about 1%.

Acknowledgements

The research is financially supported by National Natural Science Foundation of China (Grant No. U1911204，51861125203), National Key R&D Program of China (2017YFC0405900), The Project for Creative Research from Guangdong Water Resources Department (Grant No. 2018, 2020).

Declaration of competing interest The authors declare no conflicts of interest.

References

Achugbu, I.C., Olufayo, A.A., Balogun, I.A., Adefisan, E.A., Dudhia, J., Naabil, E., 2021. Modeling the spatiotemporal response of dew point temperature, air temperature and rainfall to land use land cover change over West Africa. Model. Earth Syst. Environ. https://doi.org/10.1007/s40808-021-01094-8

Ahluwalia, R.S., Rai, S.P., Meetei, P.N., Kumar, S., Sarangi, S., Chauhan, P., Karakoti, I., 2021. Spatial-diurnal variability of snow/glacier melt runoff in glacier regime river valley: Central Himalaya, India. Quat. Int. https://doi.org/https://doi.org/10.1016/j.quaint.2021.01.003

Cha, Y., Park, S.S., Kim, K., Byeon, M., Stow, C.A., 2014. Water Resources Research 5375–5377. https://doi.org/10.1002/2013WR014979.Reply

Chen, H., Chen, Y., Li, W., Li, Z., 2019. Quantifying the contributions of snow/glacier meltwater to river runoff in the Tianshan Mountains, Central Asia. Glob. Planet. Change 174, 47–57. https://doi.org/https://doi.org/10.1016/j.gloplacha.2019.01.002

Dong, Z., Brahney, J., Kang, S., Elser, J., Wei, T., Jiao, X., Shao, Y., 2020. Aeolian dust transport, cycle and influences in high-elevation cryosphere of the Tibetan Plateau region: New evidences from alpine snow and ice. Earth-Science Rev. 211, 103408. https://doi.org/https://doi.org/10.1016/j.earscirev.2020.103408

Fan, Y., Chen, Y., Li, X., Li, W., Li, Q., 2015. Characteristics of water isotopes and ice-snowmelt quantification in the Tizinafu River, north Kunlun Mountains, Central Asia. Quat. Int. 380–381, 116–122. https://doi.org/https://doi.org/10.1016/j.quaint.2014.05.020

Farrington, J.D., Tsering, D., 2019. Human-snow leopard conflict in the Chang Tang region of Tibet, China. Biol. Conserv. 237, 504–513. https://doi.org/https://doi.org/10.1016/j.biocon.2019.07.017

Gao, Z., Niu, F., Wang, Y., Lin, Z., Wang, W., 2021. Suprapermafrost groundwater flow and exchange around a thermokarst lake on the Qinghai–Tibet Plateau, China. J. Hydrol. 593, 125882. https://doi.org/https://doi.org/10.1016/j.jhydrol.2020.125882

Hall, D.K., O'Leary, D.S., DiGirolamo, N.E., Miller, W., Kang, D.H., 2021. The role of declining snow cover in the desiccation of the Great Salt Lake, Utah, using MODIS data. Remote Sens. Environ. 252, 112106. https://doi.org/https://doi.org/10.1016/j.rse.2020.112106

Jabbar, A., Othman, A.A., Merkel, B., Hasan, S.E., 2020. Change detection of glaciers and snow cover and temperature using remote sensing and GIS: A case study of the Upper Indus Basin, Pakistan. Remote Sens. Appl. Soc. Environ. 18, 100308. https://doi.org/https://doi.org/10.1016/j.rsase.2020.100308

Jia, Z., Li, P., Wu, Y., Yang, S., Wang, C., Wang, B., Yang, L., Wang, X., Li, J., Peng, Z., Guo, L., Liu, W., Liu, L., 2021. Deepened snow cover alters biotic and abiotic controls on nitrogen loss during non-growing season in temperate grasslands. Biol. Fertil. Soils 57, 165–177. https://doi.org/10.1007/s00374-020-01514-4

Jiang, W., Lü, Y., Liu, Y., Gao, W., 2020. Ecosystem service value of the Qinghai-Tibet Plateau significantly increased during 25 years. Ecosyst. Serv. 44, 101146. https://doi.org/https://doi.org/10.1016/j.ecoser.2020.101146

Konya, K., Yamaguchi, M., Takigawa, M., Miyakawa, T., O'Neel, S., 2020. Mass concentration and origin of black carbon in spring snow on glaciers in the Alaska Range. Polar Sci. 100572. https://doi.org/https://doi.org/10.1016/j.polar.2020.100572

Li, C., Yan, F., Kang, S., Yan, C., Hu, Z., Chen, P., Gao, S., Zhang, C., He, C., Kaspari, S., Stubbins, A., 2021. Carbonaceous matter in the atmosphere and glaciers of the Himalayas

and the Tibetan plateau: An investigative review. Environ. Int. 146, 106281. https://doi.org/https://doi.org/10.1016/j.envint.2020.106281

Liu, W., Xie, C., Zhao, L., Li, R., Liu, G., Wang, W., Liu, H., Wu, T., Yang, G., Zhang, Y., Zhao, S., 2021. Rapid expansion of lakes in the endorheic basin on the Qinghai-Tibet Plateau since 2000 and its potential drivers. CATENA 197, 104942. https://doi.org/https://doi.org/10.1016/j.catena.2020.104942

Niu, H., Kang, S., Wang, Y., Sarangi, C., Rupakheti, D., Qian, Y., 2020. Measurements of light-absorbing impurities in snow over four glaciers on the Tibetan Plateau. Atmos. Res. 243, 105002. https://doi.org/https://doi.org/10.1016/j.atmosres.2020.105002

Poudyal, N.C., Joshi, O., Hodges, D.G., Bhandari, H., Bhattarai, P., 2021. Climate change, risk perception, and protection motivation among high-altitude residents of the Mt. Everest region in Nepal. Ambio 50, 505–518. https://doi.org/10.1007/s13280-020-01369-x

Pu, T., Kong, Y., Wang, S., Shi, X., Wang, K., Niu, H., Chen, P., 2020. Modification of stable isotopes in snow and related post-depositional processes on a temperate glacier of Mt. Yulong, southeast Tibetan Plateau. J. Hydrol. 584, 124675. https://doi.org/https://doi.org/10.1016/j.jhydrol.2020.124675

Saarnio, S., Räty, M., Hyrkäs, M., Virkajärvi, P., 2018. Biochar addition changed the nutrient content and runoff water quality from the top layer of a grass field during simulated snowmelt. Agric. Ecosyst. Environ. 265, 156–165. https://doi.org/https://doi.org/10.1016/j.agee.2018.06.007

Shijin, W., Lanyue, Z., Yanqiang, W., 2019. Integrated risk assessment of snow disaster over the Qinghai-Tibet Plateau. Geomatics, Nat. Hazards Risk 10, 740–757. https://doi.org/10.1080/19475705.2018.1543211

Sobota, I., Weckwerth, P., Grajewski, T., 2020. Rain-On-Snow (ROS) events and their relations to snowpack and ice layer changes on small glaciers in Svalbard, the high Arctic. J. Hydrol. 590, 125279. https://doi.org/https://doi.org/10.1016/j.jhydrol.2020.125279

Sood, V., Gusain, H.S., Gupta, S., Taloor, A.K., Singh, S., 2020. Detection of snow/ice cover changes using subpixel-based change detection approach over Chhota-Shigri glacier, Western Himalaya, India. Quat. Int. https://doi.org/https://doi.org/10.1016/j.quaint.2020.05.016

Steele, C., Dialesandro, J., James, D., Elias, E., Rango, A., Bleiweiss, M., 2017. Evaluating MODIS snow products for modelling snowmelt runoff: Case study of the Rio Grande headwaters. Int. J. Appl. Earth Obs. Geoinf. 63, 234–243. https://doi.org/https://doi.org/10.1016/j.jag.2017.08.007

Sun, X., Zhang, R., Huang, W., Sun, A., Lin, L., Xu, H., Jiang, D., 2019. The response between glacier evolution and eco-geological environment on the Qinghai-Tibet Plateau. China Geol. 2, 1–7. https://doi.org/https://doi.org/10.31035/cg2018078

Tang, Z., Wang, Xiaoru, Deng, G., Wang, Xin, Jiang, Z., Sang, G., 2020. Spatiotemporal variation of snowline altitude at the end of melting season across High Mountain Asia, using MODIS snow cover product. Adv. Sp. Res. 66, 2629–2645. https://doi.org/https://doi.org/10.1016/j.asr.2020.09.035

Teng, Y., Zhan, J., Liu, W., Sun, Y., Agyemang, F.B., Liang, L., Li, Z., 2021. Spatiotemporal dynamics and drivers of wind erosion on the Qinghai-Tibet Plateau, China. Ecol. Indic. 123, 107340. https://doi.org/https://doi.org/10.1016/j.ecolind.2021.107340

Thapa, P., Xu, J., Neupane, B., Rupakheti, D., 2020. Chemical composition of inorganic and organic species in snow/ice in the glaciers of western China. Sci. Total Environ. 706, 135351. https://doi.org/https://doi.org/10.1016/j.scitotenv.2019.135351

Thind, P.S., Kumar, D., John, S., 2021. Source apportionment of the light absorbing impurities present in surface snow of the India Western Himalayan glaciers. Atmos. Environ. 246, 118173. https://doi.org/https://doi.org/10.1016/j.atmosenv.2020.118173

Tong, R., Parajka, J., Komma, J., Blöschl, G., 2020. Mapping snow cover from daily Collection 6 MODIS products over Austria. J. Hydrol. 590, 125548. https://doi.org/https://doi.org/10.1016/j.jhydrol.2020.125548

Wang, Y., Quan, Q., Shen, B., 2019. Spatio-temporal variability of drought and effect of large scale climate in the source region of Yellow River. Geomatics, Nat. Hazards Risk 10, 678–698. https://doi.org/10.1080/19475705.2018.1541827

Wen, Z., Song, K., Liu, G., Shang, Y., Hou, J., Lyu, L., Fang, C., 2019. Impact factors of dissolved organic carbon and the transport in a river-lake continuum in the Tibet Plateau of China. J. Hydrol. 579, 124202. https://doi.org/https://doi.org/10.1016/j.jhydrol.2019.124202

Wu, Y., Ouyang, W., Hao, Z., Yang, B., Wang, L., 2018. Snowmelt water drives higher soil erosion than rainfall water in a mid-high latitude upland watershed. J. Hydrol. 556, 438–448. https://doi.org/https://doi.org/10.1016/j.jhydrol.2017.11.037

Xiaohua, H.A.O., 2019. Long time series data of snow cover area on Qinghai-Tibet Plateau (2003-2014). Natl. Tibet. Plateau Data Cent. https://doi.org/10.11888/Snow.tpdc.270471

Yang, Y., Weng, B., Man, Z., Yu, Z., Zhao, J., 2020. Analyzing the contributions of climate change and human activities on runoff in the Northeast Tibet Plateau. J. Hydrol. Reg. Stud. 27, 100639. https://doi.org/https://doi.org/10.1016/j.ejrh.2019.100639

Yi, Y., Liu, S., Zhu, Y., Wu, K., Xie, F., Saifullah, M., 2021. Spatiotemporal heterogeneity of snow cover in the central and western Karakoram Mountains based on a refined MODIS product during 2002–2018. Atmos. Res. 250, 105402. https://doi.org/https://doi.org/10.1016/j.atmosres.2020.105402

Yu, Z., Gu, H., Wang, J., Xia, J., Lu, B., 2018. Effect of projected climate change on the hydrological regime of the Yangtze River Basin, China. Stoch. Environ. Res. Risk Assess. 32, 1–16. https://doi.org/10.1007/s00477-017-1391-2

Zhang, B., Chen, T., Guo, J., Wu, M., Yang, R., Chen, X., Wu, X., Zhang, W., Kang, S., Liu, G., Dyson, P., 2020. Microbial mercury methylation profile in terminus of a high-elevation glacier on the northern boundary of the Tibetan Plateau. Sci. Total Environ. 708, 135226. https://doi.org/https://doi.org/10.1016/j.scitotenv.2019.135226

Zhang, H., Zhang, F., Zhang, G., Che, T., Yan, W., Ye, M., Ma, N., 2019. Ground-based evaluation of MODIS snow cover product V6 across China: Implications for the selection of NDSI threshold. Sci. Total Environ. 651, 2712–2726. https://doi.org/https://doi.org/10.1016/j.scitotenv.2018.10.128

Zhang, H., Zhang, F., Zhang, G., Yan, W., Li, S., 2021. Enhanced scaling effects significantly lower the ability of MODIS normalized difference snow index to estimate fractional and binary snow cover on the Tibetan Plateau. J. Hydrol. 592, 125795. https://doi.org/https://doi.org/10.1016/j.jhydrol.2020.125795

Zhang, J., Jiang, F., Li, G., Qin, W., Wu, T., Xu, F., Hou, Y., Song, P., Cai, Z., Zhang, T., 2021. The four antelope species on the Qinghai-Tibet plateau face habitat loss and redistribution to

539 higher latitudes under climate change. Ecol. Indic. 123, 107337.
540 https://doi.org/https://doi.org/10.1016/j.ecolind.2021.107337
541 Zhang, W., Shen, Y., Wang, X., Kang, S., Chen, A., Mao, W., Zhong, X., 2021. Snow cover
542 controls seasonally frozen ground regime on the southern edge of Altai Mountains. Agric.
543 For. Meteorol. 297, 108271. https://doi.org/https://doi.org/10.1016/j.agrformet.2020.108271
544 Zhang, X., Wang, H., Che, H.-Z., Tan, S.-C., Shi, G.-Y., Yao, X.-P., Zhao, H.-J., 2020.
545 Improvement of snow/haze confusion data gaps in MODIS Dark Target aerosol retrievals in
546 East China. Atmos. Res. 245, 105063.
547 https://doi.org/https://doi.org/10.1016/j.atmosres.2020.105063
548 Zhao, G., Li, W., Li, F., Zhang, F., Liu, G., 2018. Hydrochemistry of waters in snowpacks, lakes
549 and streams of Mt. Dagu, eastern of Tibet Plateau. Sci. Total Environ. 610–611, 641–650.
550 https://doi.org/https://doi.org/10.1016/j.scitotenv.2017.08.088
551 Zhou, Y., Li, Z., Li, J., Zhao, R., Ding, X., 2018. Glacier mass balance in the Qinghai–Tibet
552 Plateau and its surroundings from the mid-1970s to 2000 based on Hexagon KH-9 and
553 SRTM DEMs. Remote Sens. Environ. 210, 96–112.
554 https://doi.org/https://doi.org/10.1016/j.rse.2018.03.020
555 Zhu, J., Shi, J., Wang, Y., 2012. Subpixel snow mapping of the Qinghai–Tibet Plateau using
556 MODIS data. Int. J. Appl. Earth Obs. Geoinf. 18, 251–262.
557 https://doi.org/https://doi.org/10.1016/j.jag.2012.02.001
558 Zhu, Y., Ishikawa, T., Siva Subramanian, S., Luo, B., 2021. Early warning system for rainfall- and
559 snowmelt-induced slope failure in seasonally cold regions. Soils Found.
560 https://doi.org/https://doi.org/10.1016/j.sandf.2020.11.009
561

Figures

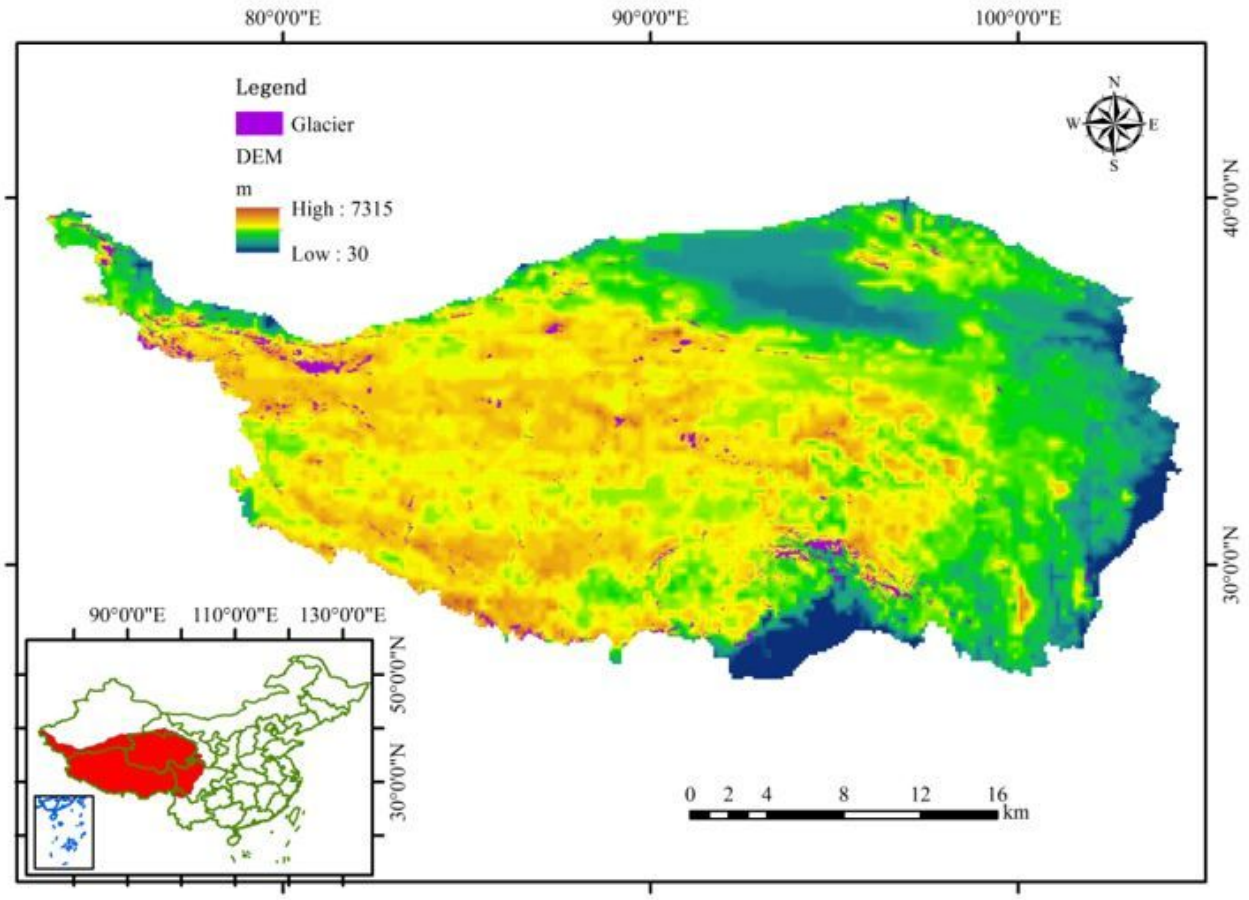

Figure 1

Location of study area and distribution of glaciers Note: The designations employed and the presentation of the material on this map do not imply the expression of any opinion whatsoever on the part of Research Square concerning the legal status of any country, territory, city or area or of its authorities, or concerning the delimitation of its frontiers or boundaries. This map has been provided by the authors.

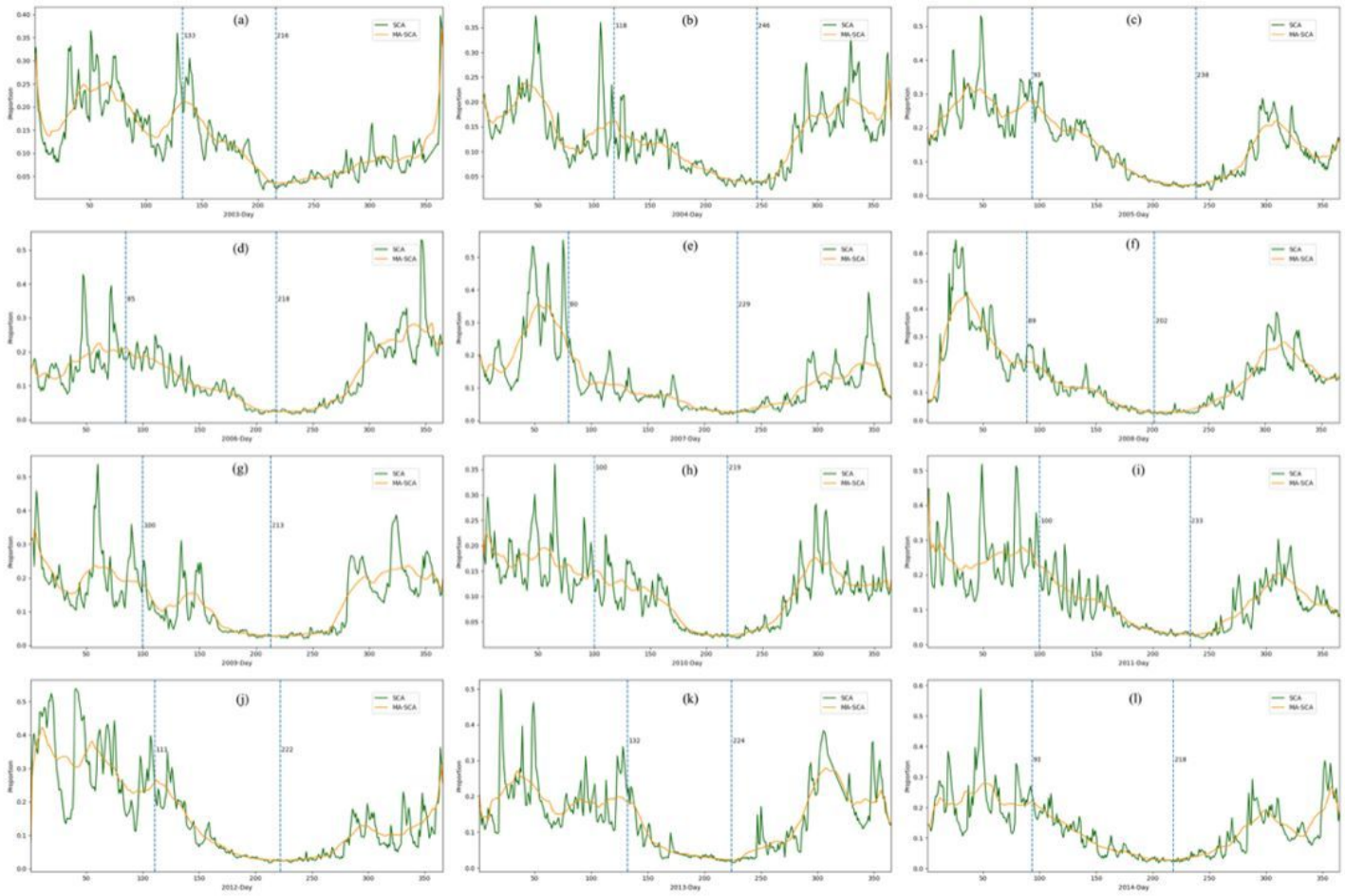

Figure 2

Changes in daily snow cover area of the TP from 2003 to 2014 (a-l: 2003-2014)

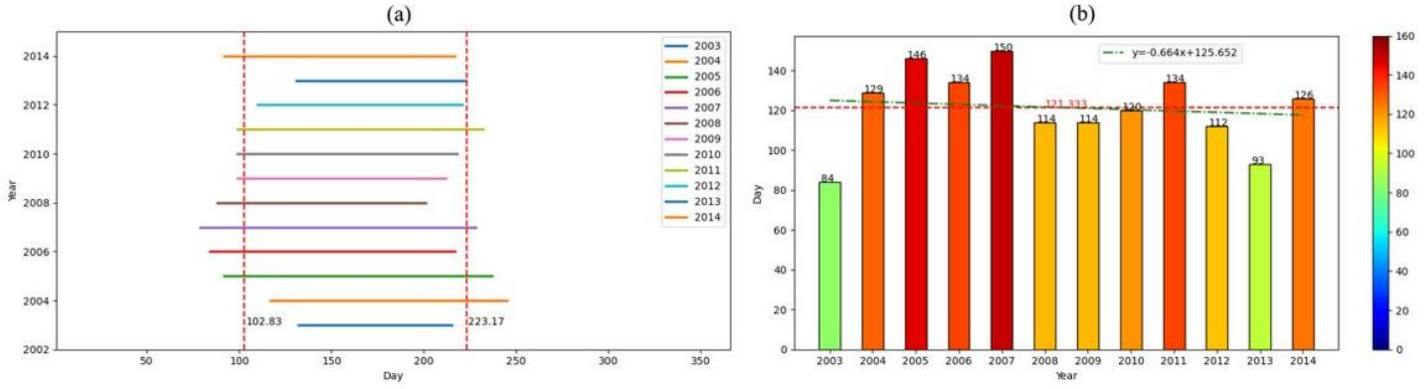

Figure 3

Snowmelt duration time (a) and change trend (b) from 2003 to 2014

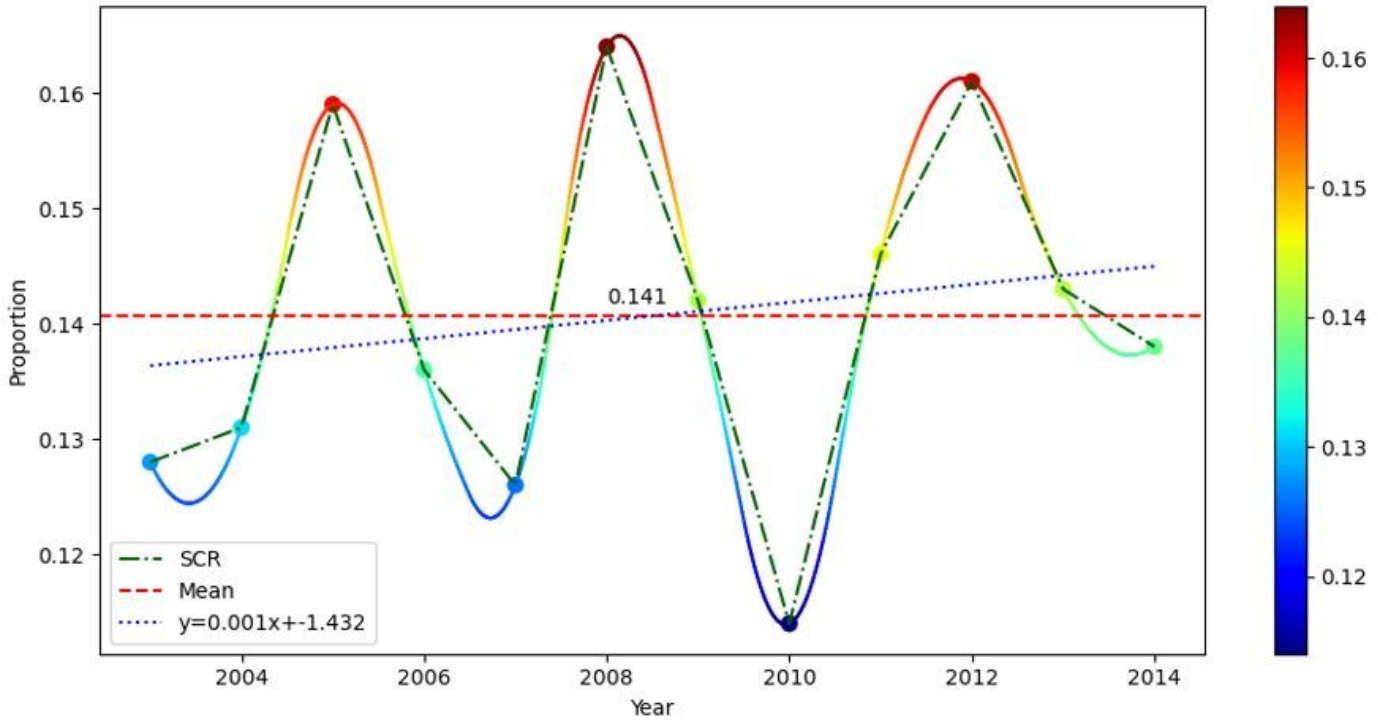

Figure 4

Changes in the average annual SCR from 2003 to 2014

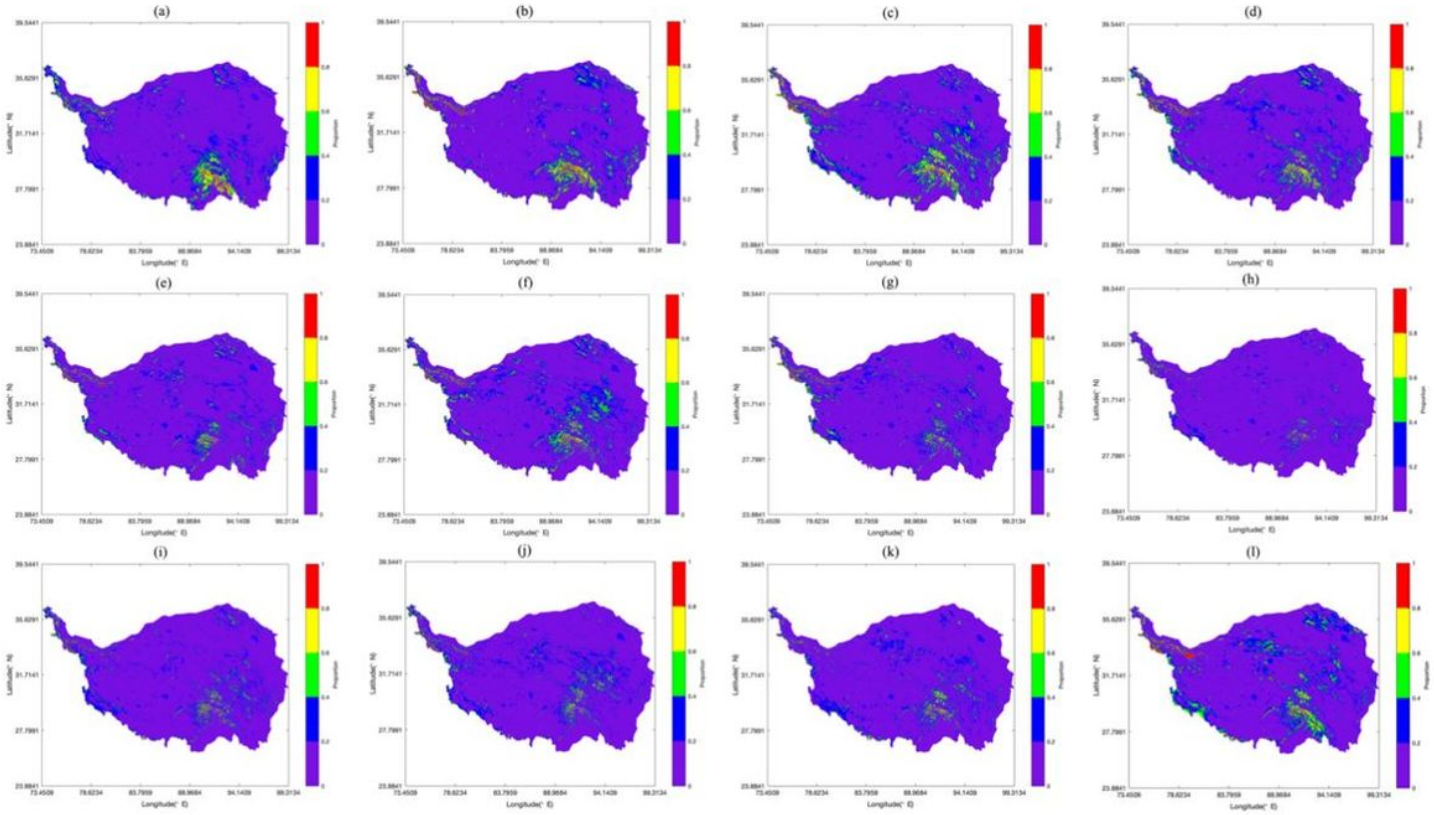

Figure 5

Distribution of average annual SCR from 2003 to 2014 in the TP (a-l: 2003-2004) Note: The designations employed and the presentation of the material on this map do not imply the expression of any opinion whatsoever on the part of Research Square concerning the legal status of any country, territory, city or area or of its authorities, or concerning the delimitation of its frontiers or boundaries. This map has been provided by the authors.

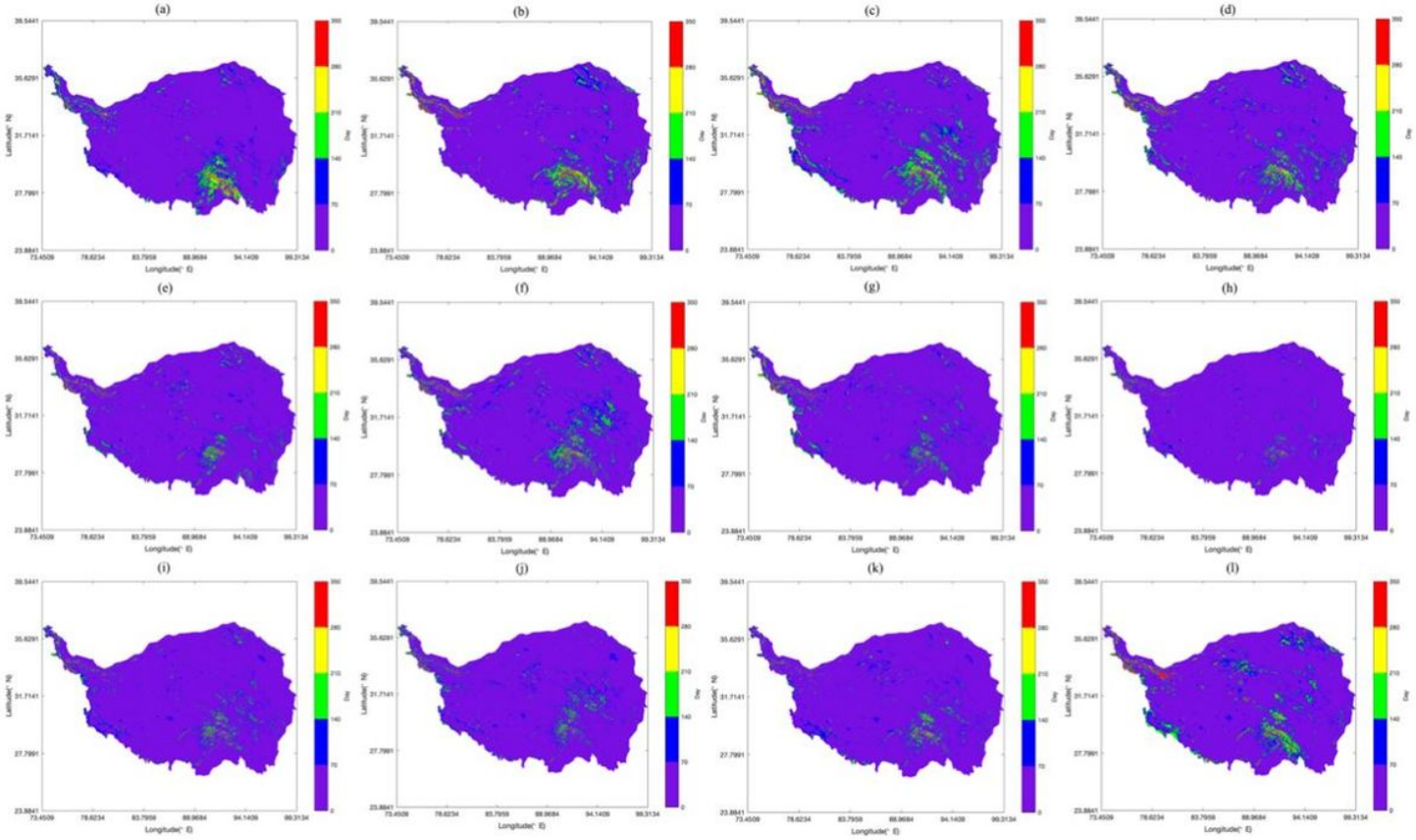

Figure 6

Spatial distribution of annual SCD on the TP from 2003 to 2014 (a-l: 2003-2014) Note: The designations employed and the presentation of the material on this map do not imply the expression of any opinion whatsoever on the part of Research Square concerning the legal status of any country, territory, city or area or of its authorities, or concerning the delimitation of its frontiers or boundaries. This map has been provided by the authors.

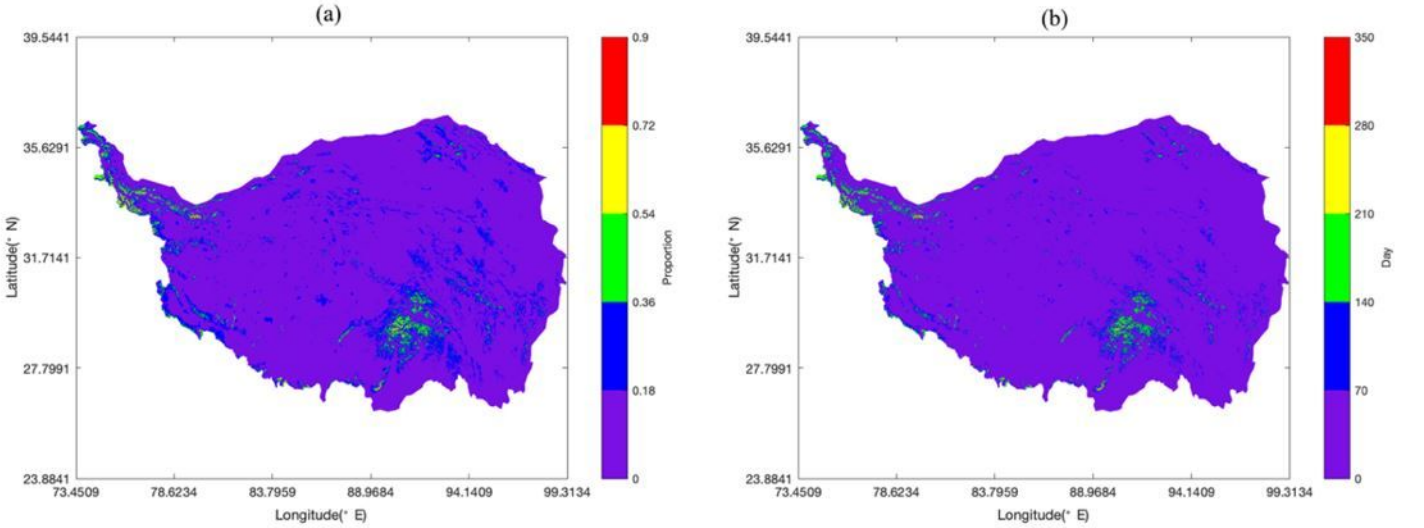

Figure 7

Spatial distribution of the multi-year average SCR (a) and SCD (b) on the TP Note: The designations employed and the presentation of the material on this map do not imply the expression of any opinion whatsoever on the part of Research Square concerning the legal status of any country, territory, city or area or of its authorities, or concerning the delimitation of its frontiers or boundaries. This map has been provided by the authors.

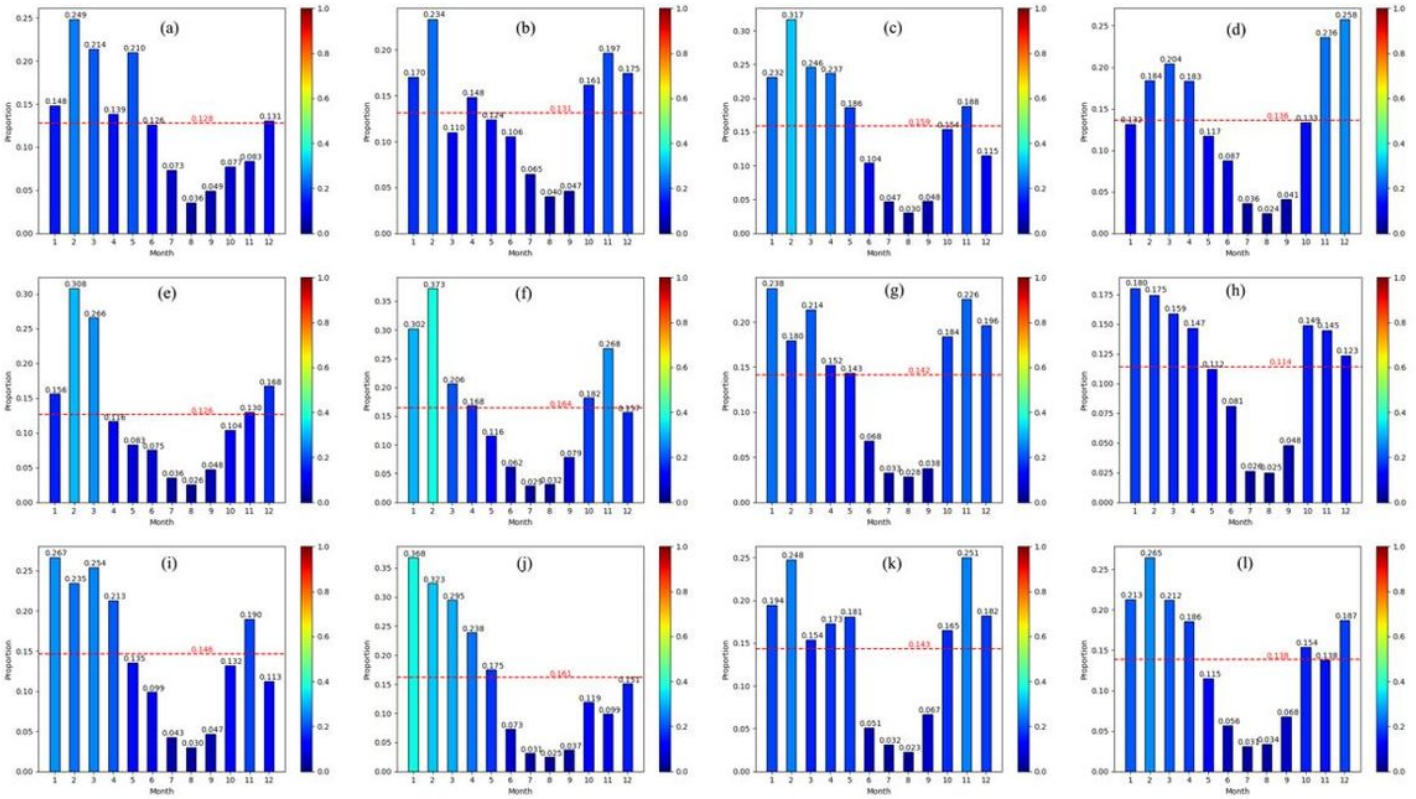

Figure 8

Monthly SCR change from 2003 to 2014 (a-l, 2003-2014)

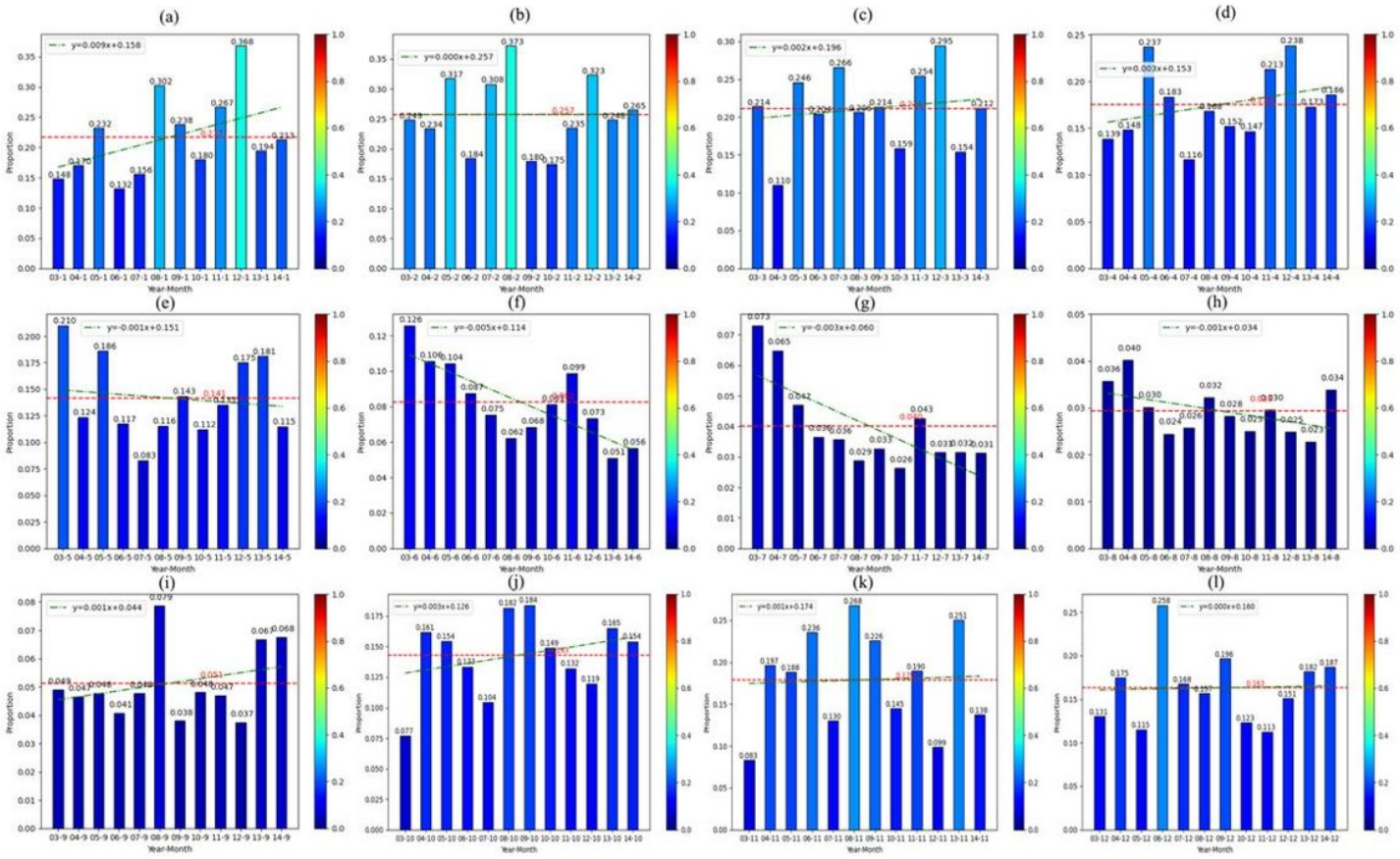

Figure 9

Changes in SCR of TP from January to December (a-l: Jan-Dec)

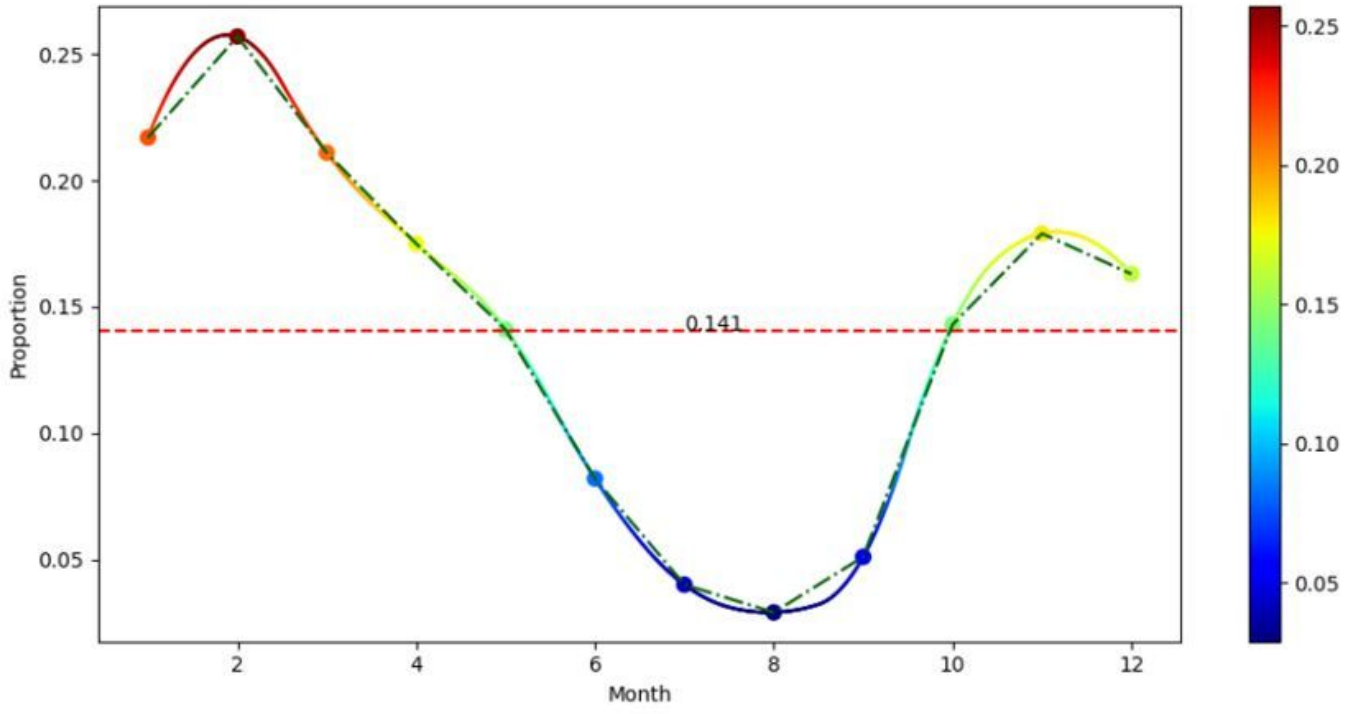

Figure 10

Changes in monthly average SCR on the TP

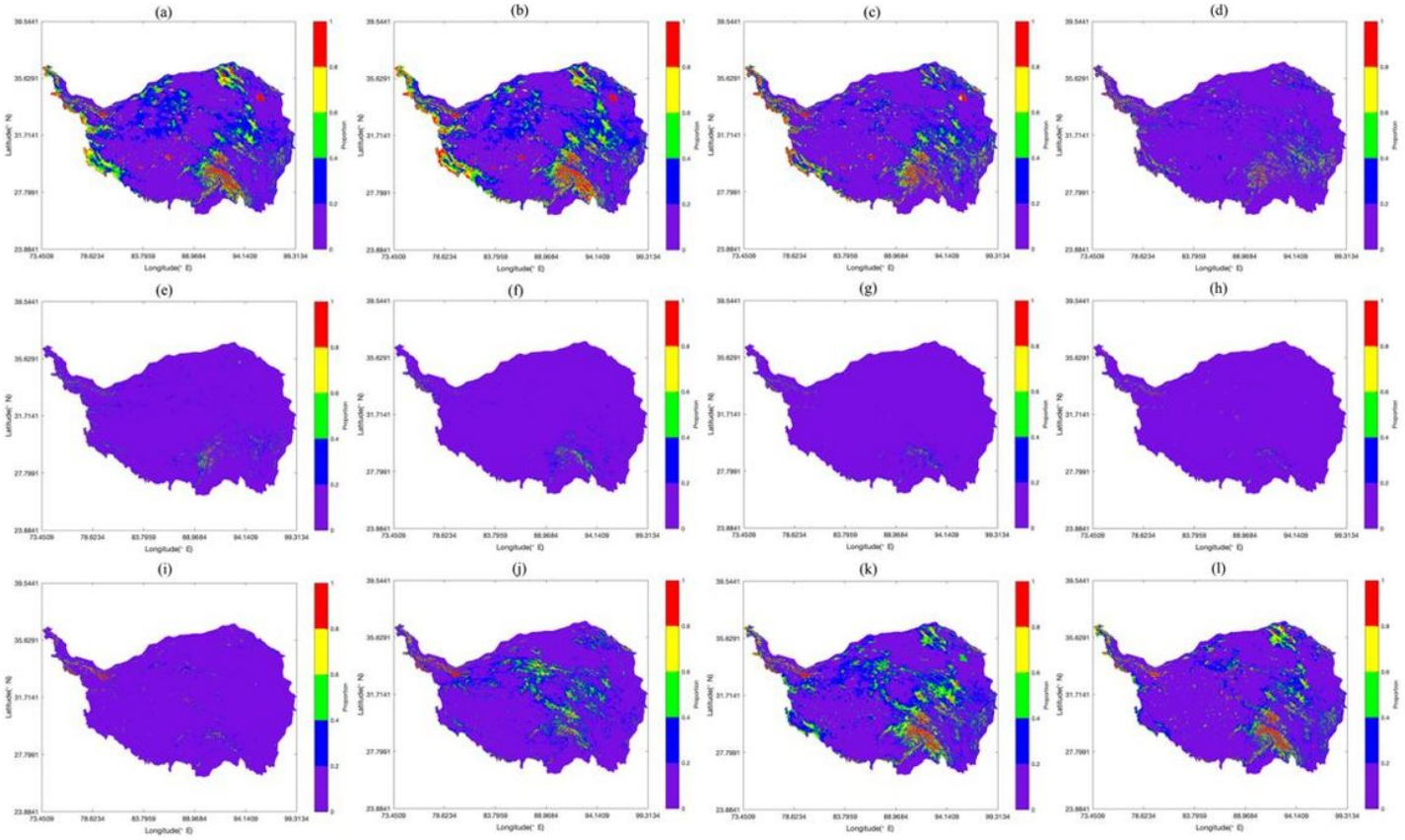

Figure 11

Spatial distribution of monthly average SCR on TP from January to December (a-l: Jan-Dec) Note: The designations employed and the presentation of the material on this map do not imply the expression of any opinion whatsoever on the part of Research Square concerning the legal status of any country, territory, city or area or of its authorities, or concerning the delimitation of its frontiers or boundaries. This map has been provided by the authors.

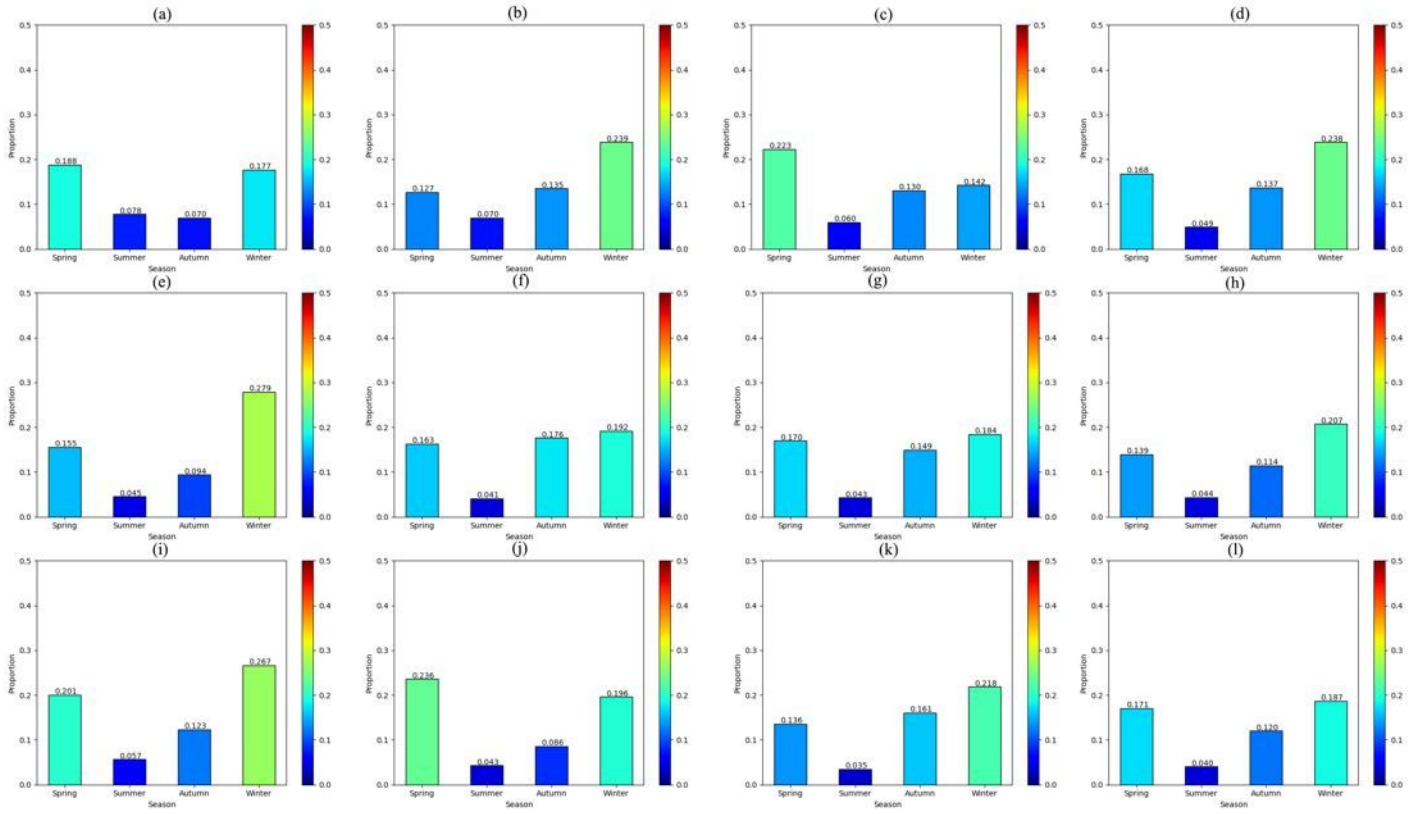

Figure 12

Seasonal change of SCR on TP from 2003 to 2014 (a-l: 2003-2014)

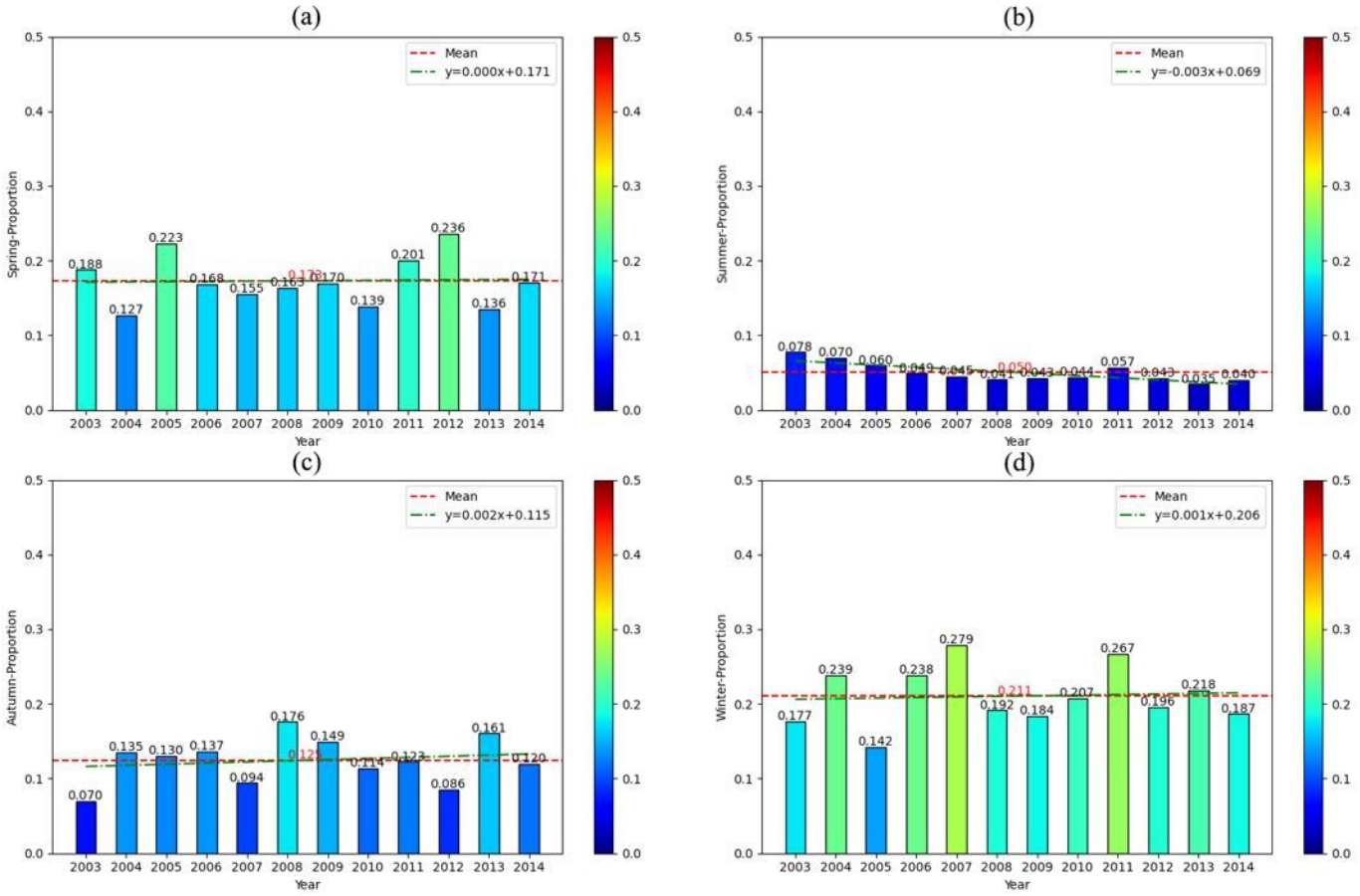

Figure 13

Changes in SCR of the TP from 2003 to 2014 in spring (a), summer (b), autumn (c) and winter (d)

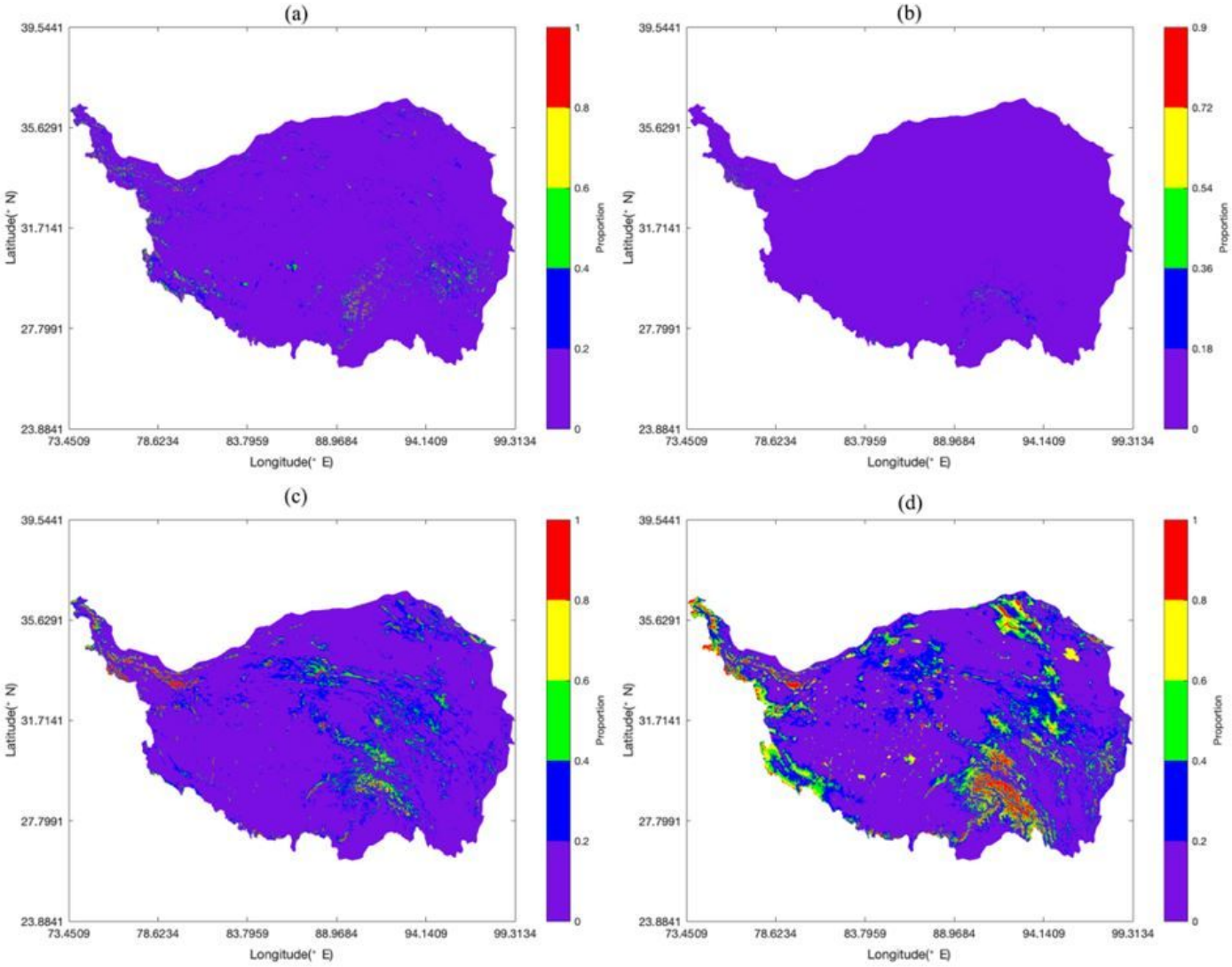

Figure 14

Spatial distribution of average SCR in spring (a), summer (b), autumn (c) and winter (d) on the TP Note: The designations employed and the presentation of the material on this map do not imply the expression of any opinion whatsoever on the part of Research Square concerning the legal status of any country, territory, city or area or of its authorities, or concerning the delimitation of its frontiers or boundaries. This map has been provided by the authors.

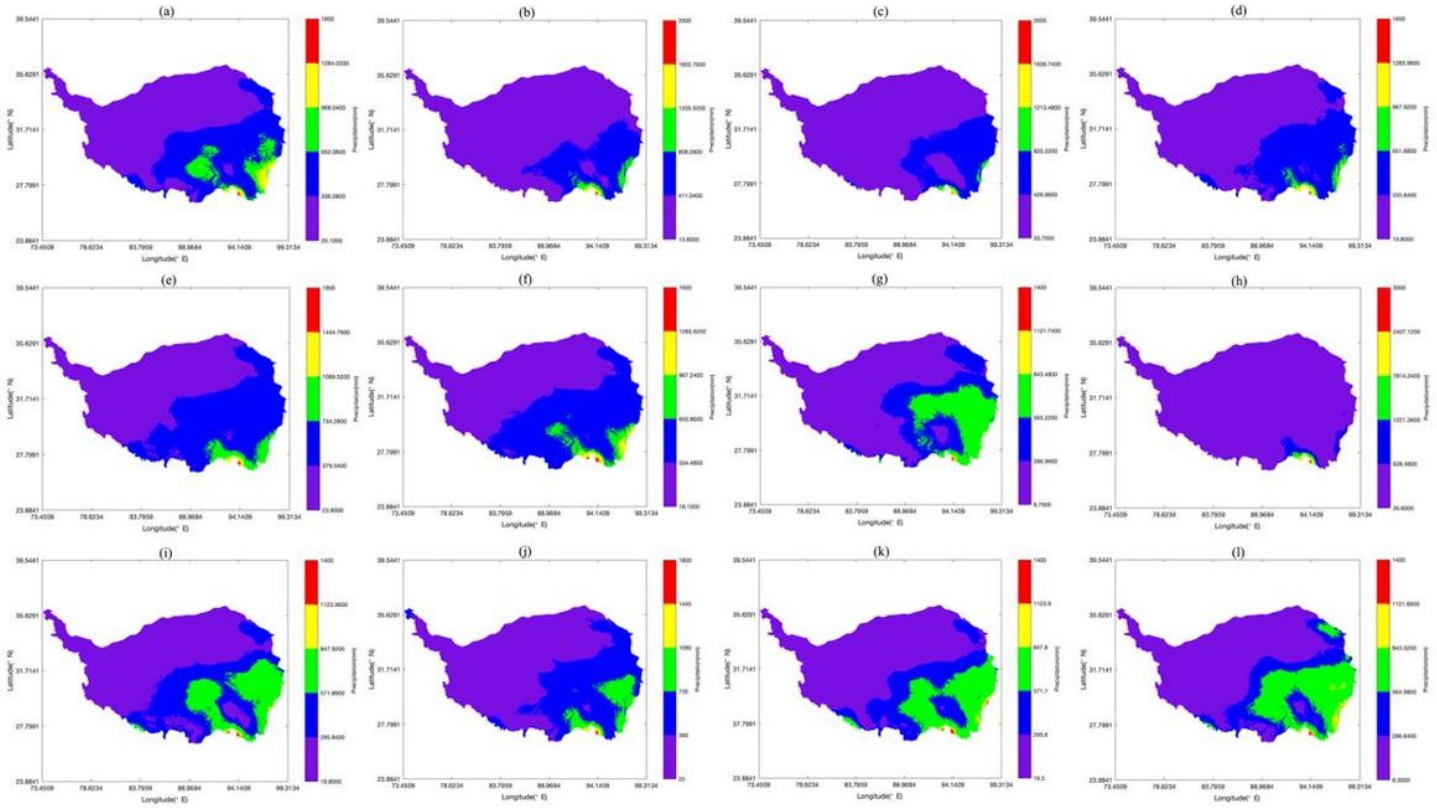

Figure 15

Spatial distribution of annual precipitation on the TP from 2003 to 2014 (a-l: 2003-2014) Note: The designations employed and the presentation of the material on this map do not imply the expression of any opinion whatsoever on the part of Research Square concerning the legal status of any country, territory, city or area or of its authorities, or concerning the delimitation of its frontiers or boundaries. This map has been provided by the authors.

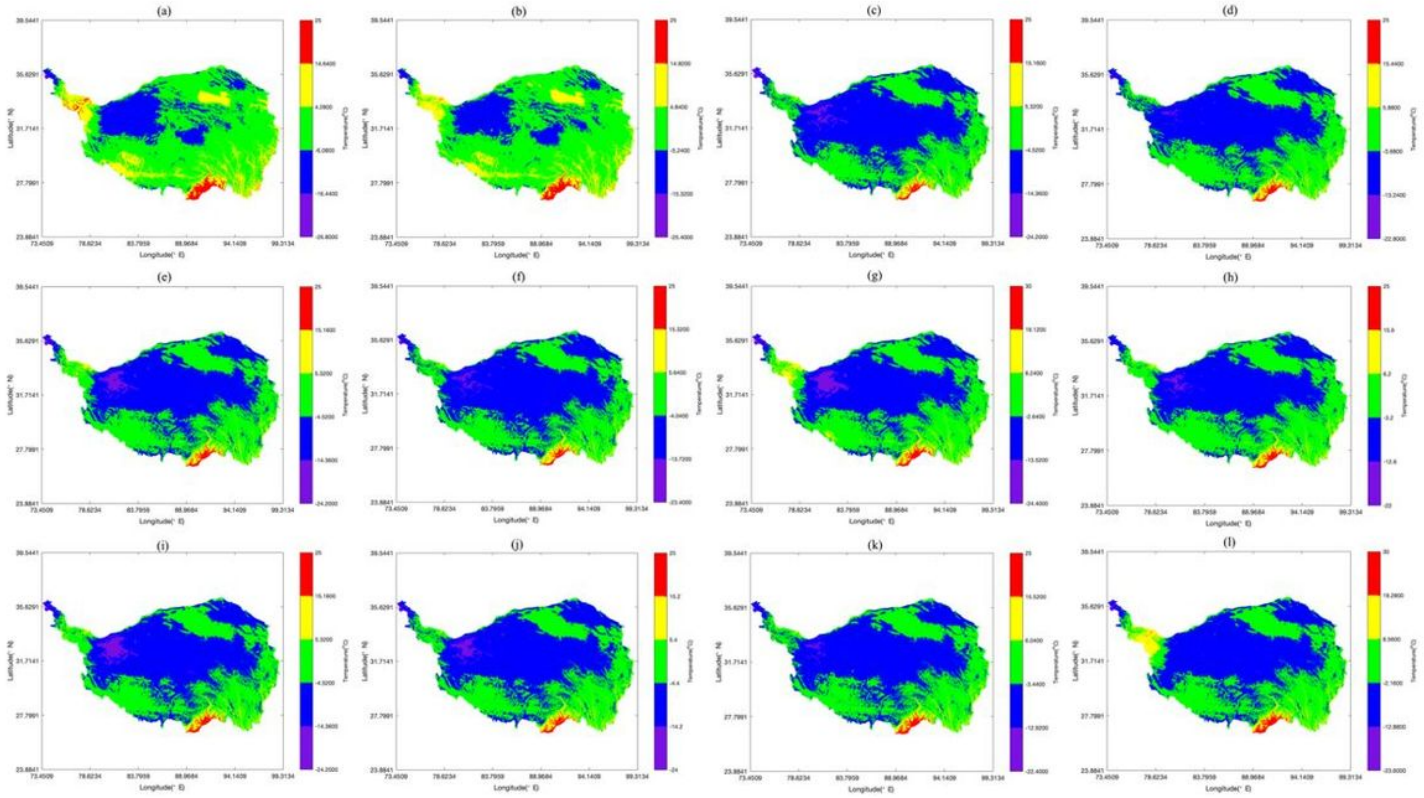

Figure 16

Spatial distribution of annual average temperature on the TP from 2003 to 2014 (a-l: 2003-2014) Note: The designations employed and the presentation of the material on this map do not imply the expression of any opinion whatsoever on the part of Research Square concerning the legal status of any country, territory, city or area or of its authorities, or concerning the delimitation of its frontiers or boundaries. This map has been provided by the authors.

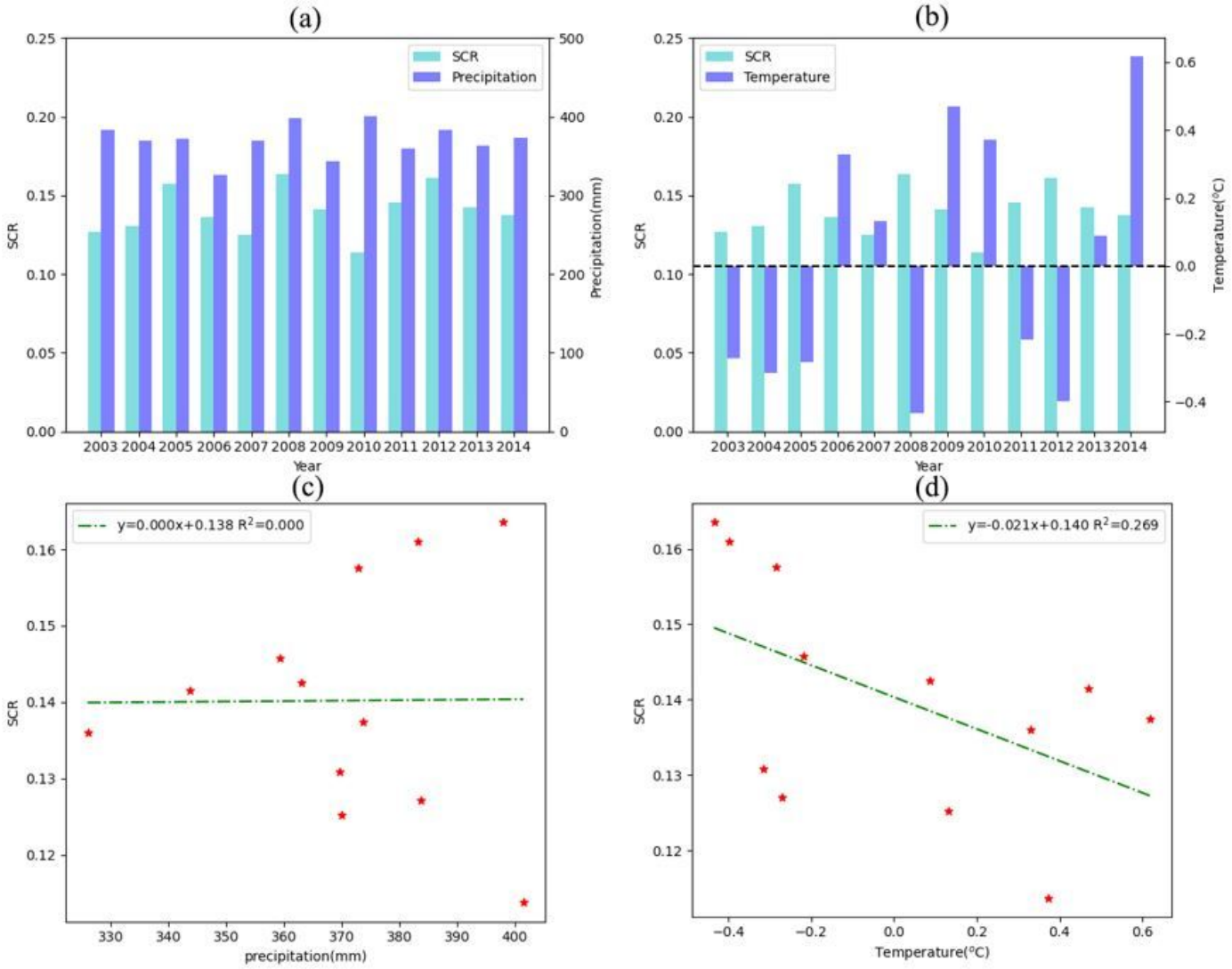

Figure 17

Changes of SCR with precipitation (a) and temperature (b) from 2003 to 2014, and correlations of SCR with precipitation (c) and temperature (d)

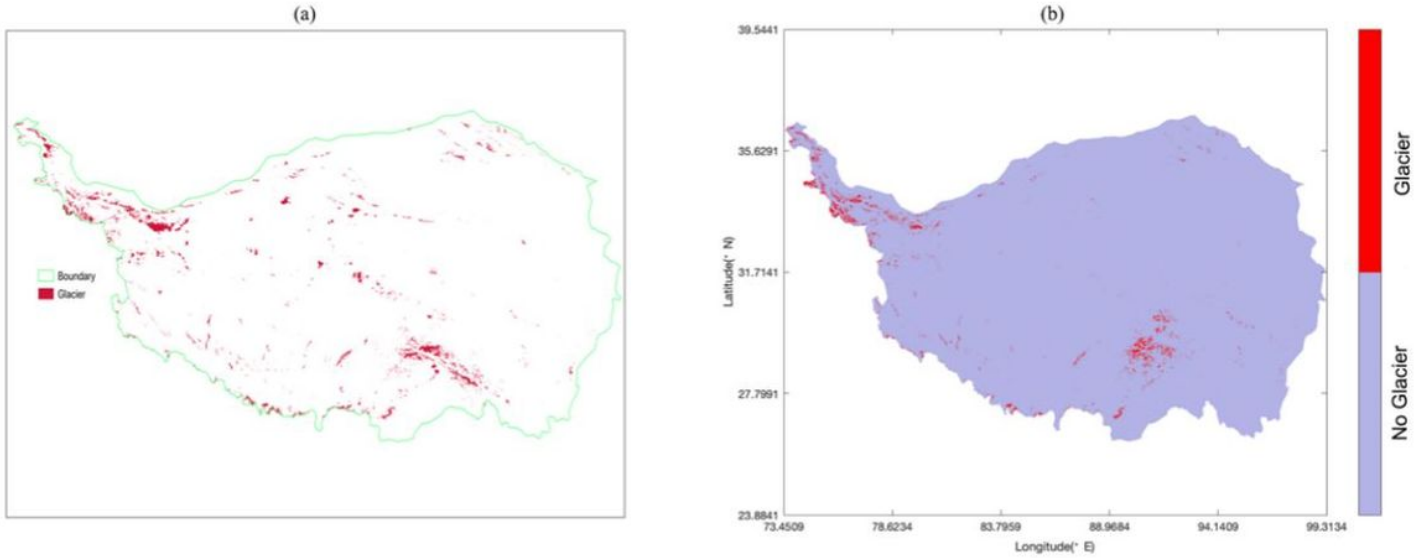

Figure 18

Glacier cover on the TP based on RGI (a) and SCR (b) Note: The designations employed and the presentation of the material on this map do not imply the expression of any opinion whatsoever on the part of Research Square concerning the legal status of any country, territory, city or area or of its authorities, or concerning the delimitation of its frontiers or boundaries. This map has been provided by the authors.